Identification of novel TMPRSS2:ERG mechanisms in prostate cancer metastasis: involvement of MMP9 and PLXNA2

T V Tian, N Tomavo, L Huot, A Flourens, E Bonnelye, S Flajollet, D. Hot, X Leroy, Y de Launoit, M. Duterque-Coquillaud

▶ **To cite this version:**

T V Tian, N Tomavo, L Huot, A Flourens, E Bonnelye, et al.. Identification of novel TMPRSS2:ERG mechanisms in prostate cancer metastasis: involvement of MMP9 and PLXNA2. Oncogene, 2014, 33 (17), pp.2204-2214. 10.1038/onc.2013.176 . hal-02353391

HAL Id: hal-02353391
https://hal.science/hal-02353391

Submitted on 8 Nov 2019

HAL is a multi-disciplinary open access archive for the deposit and dissemination of scientific research documents, whether they are published or not. The documents may come from teaching and research institutions in France or abroad, or from public or private research centers.

L'archive ouverte pluridisciplinaire **HAL**, est destinée au dépôt et à la diffusion de documents scientifiques de niveau recherche, publiés ou non, émanant des établissements d'enseignement et de recherche français ou étrangers, des laboratoires publics ou privés.

Identification of novel TMPRSS2:ERG mechanisms in prostate cancer metastasis: involvement of MMP9 and PLXNA2

Tian V. Tian[1,2,3,4], Nathalie Tomavo[1,2,3], Ludovic Huot[2,3,5], Anne Flourens[1,2,3], Edith Bonnelye[6], Sébastien Flajollet[1,2,3], David Hot[2,3,5], Xavier Leroy[3,4,7], Yvan de Launoit[1,2,3], Martine Duterque-Coquillaud[1,2,3]

[1]Institut de Biologie de Lille, CNRS UMR8161, Lille, France; [2]Institut Pasteur de Lille / IFR142, Lille, France; [3]Université de Lille Nord de France, Lille, France; [4]Faculté de Médecine Henri Warembourg, Université du Droit et de la Santé Lille II, Lille, France; [5]Centre d'Infection et d'Immunité de Lille (CIIL), INSERM U1019, CNRS UMR8204, Lille, France; [6]INSERM U1033, Lyon, France; [7]Centre hospitalier régional et universitaire de Lille, Institut de Pathologie, Lille, France

Correspondance: Dr. Martine Duterque-Coquillaud, Institut de Biologie de Lille, CNRS UMR8161, 1 rue du Professeur Calmette, F59021, France

Email: martine.duterque@ibl.fr

Telephone: +33 3 20 87 10 95

Fax: +33 3 20 87 11 11

Running title: TMPRSS2:ERG regulates MMP9 and PLXNA2

ABSTRACT

Prostate cancer (PCa) is one of the major public health problems in Western countries. Recently, the *TMPRSS2:ERG* gene fusion, which results in the aberrant expression of the transcription factor ERG, has been shown to be the most common gene rearrangement in PCa. Previous studies have determined the contributions of this fusion in PCa disease initiation and/or progression *in vitro* and *in vivo*. In this study on TMPRSS2:ERG regulation in PCa, we used an androgen receptor (AR) and *TMPRSS2:ERG* fusion double-negative prostate cancer cell model: PC3c. In three cell clones with different *TMPRSS2:ERG* expression levels, ectopic expression of the fusion resulted in significant induction of cell migration and invasion in a dose-dependent manner. In agreement with this phenotype, high-throughput microarray analysis revealed that a set of genes, functionally associated with cell motility and invasiveness, were deregulated in a dose-dependent manner in *TMPRSS2:ERG*-expressing cells. Importantly, we identified increased *MMP9* and *PLXNA2* expression in *TMPRSS2:ERG*-positive PCa samples, and their expression levels were significantly correlated with *ERG* expression in a PCa cohort. In line with these findings, there was evidence that TMPRSS2:ERG directly and positively regulates MMP9 and PLXNA2 expression in PC3c cells. Moreover, PLXNA2 upregulation contributed to *TMPRSS2:ERG*-mediated enhancements of PC3c cell migration and invasion. Furthermore, and importantly, *PLXNA2* expression was upregulated in metastatic PCa tumors compared to localized primary PCa tumors. This study provides novel insights into the role of the *TMPRSS2:ERG* fusion in PCa metastasis.

Key words: Prostate cancer, *TMPRSS2:ERG* fusion, Migration, Invasion, MMP9, PLXNA2.

INTRODUCTION

Prostate cancer (PCa) is one of the most prevalent malignancies and a leading cause of cancer-related deaths affecting men in Western countries (1). Recent PCa cytogenetic and genomic studies have highlighted several critical genomic alterations involved in disease onset and/or progression (2). Of these, genomic rearrangements leading to the aberrant expression of the E-twenty-six (*ETS*) family of transcription factors in PCa is considered as a hallmark (3, 4). The most frequent genomic rearrangement in PCa is the fusion of the ETS-related gene (*ERG*) with 5' regulatory elements of the androgen receptor (AR)-responsive transmembrane protease serine 2 (*TMPRSS2*), which has been identified in 40% to 70% of PCa patient samples (3). The *TMPRSS2:ERG* gene fusion leads to aberrant expression of full length and/or N-terminal-truncated ERG transcription factors in PCa (referred to as TMPRSS2:ERG protein in this study) (5).

The association between *TMPRSS2:ERG* fusion and PCa clinical outcome has not yet been clearly established. Some studies have shown that this gene fusion is not significantly associated with PCa disease progression or prognosis (6-8); however, other studies have demonstrated that it is associated with favorable (9, 10) or poor clinical outcomes (11-16).

Functional studies on the role of *TMPRSS2:ERG* in PCa have been performed using PCa cell lines as well as mouse models. Although some reports have demonstrated that ectopic *TMPRSS2:ERG* expression in the prostate is sufficient to induce prostatic intraepithelial neoplasia (PIN) in mice, a pre-malignancy form of PCa (17, 18), others have highlighted how *TMPRSS2:ERG* expression cooperates with other genomic alterations, such as *PTEN* haploinsufficiency, constitutive PI3K/AKT activation or AR signaling, to promote PCa cell migration, invasion and disease progression (19-21). Using next-generation sequencing technologies, recent studies aiming to identify TMPRSS2:ERG direct target genes in established PCa cell models have provided further evidence that ERG can modulate the

output of AR target genes (22-24). These studies provide functional insights into the role of TMPRSS2:ERG in PCa initiation and/or progression.

Nevertheless, PCa is considered as a multifocal disease, because primary PCa tumors are mainly composed of multiple, genetically distinct cancer cells (2, 25-27). Regarding *TMPRSS2:ERG* status and the corresponding TMPRSS2:ERG protein expression profile, a significant prevalence of inter- and/or intra-focal heterogeneity has been also observed in several PCa cohorts (28-31). This raises the possibility that the differentially expressed TMPRSS2:ERG protein can control variable transcriptional programs in genetically distinct PCa cells. It is therefore necessary to perform studies on different PCa cell models.

In this study, we examined the role of *TMPRSS2:ERG* using an established PCa cell model, PC3c, which was previously isolated from AR and *TMPRSS2:ERG* double-negative PC3 cells (32). *In vivo* studies have revealed that PC3c cells can induce mixed lesions in bone (32), a commonly observed complication in PCa patients with advanced disease (33). Here, we demonstrate that ectopic expression of *TMPRSS2:ERG* fusion increases PC3c cell migration and invasion in a dose-dependent manner. High-throughput transcriptomic studies revealed that a set of genes related to cell motility and invasiveness is deregulated in *TMPRSS2:ERG*-expressing cells in a dose-dependent manner. We further demonstrate that TMPRSS2:ERG directly and positively regulates MMP9 (Metalloproteinase 9) and PLXNA2 (Plexin A2) expression in PC3c cells, and that PLXNA2 upregulation contributes to the *TMPRSS2:ERG*-mediated PC3c cell migration and invasion.

RESULTS

Ectopic TMPRSS2:ERG expression leads to phenotype changes in PC3c cells.

Previous studies have identified diverse *TMPRSS2:ERG* fusion transcripts in human PCa samples, and the most frequent variant is composed of exon 1 of the *TMPRSS2* gene (NM_005656) fused to exon 4 of the *ERG* gene (NM_004449) (5, 34). In addition, the presence of a 72bp exon in fusion gene transcripts may contribute to a more aggressive phenotype (35). We therefore used the *TMPRSS2:ERG* fusion isoform that includes exon 1 of *TMPRSS2* fused to exon 4 of *ERG* with the presence of the 72bp exon (Figure 1a).

Three *TMPRSS2:ERG*-expressing clones were included in this study, designated as H clone (high), M clone (moderate) and L clone (low), according to their *ERG* mRNA expression levels (Figure 1b). *ERG* mRNA levels in H cells were 2-fold and 10-fold higher than in M cells and in L cells respectively, whereas no endogenous *ERG* mRNA was found in pcDNA control cells or in parental PC3c cells. In particular, *ERG* expression in H cells was only about 50% of that in VCaP cells (endogenous *TMPRSS2:ERG*-expressing PCa cells), and comparable to endogenous full-length *ERG* expression in HUVEC cells, suggesting that *TMPRSS2:ERG* expression levels in our cell models were not excessive. As expected, high, moderate and low expression levels of TMPRSS2:ERG protein were only found respectively in H, M and L cells, and not in control cells or in parental PC3c cells (Figure 1c). In addition, compared to VCaP cells, TMPRSS2:ERG expression in H cells was lower (Supplementary Figure S1).

A comparison of H, M and L cell morphology to that of control cells showed that, where control cells were round and clustered, H cells were more elongated and scattered (Figure 2a). This morphological change was also observed, to a lesser extent, in M cells, but nearly absent in L cells (Figure 2a). Next, we examined whether the ectopic *TMPRSS2:ERG* expression could have an impact on PC3c cell proliferation. Surprisingly, no significant cell proliferation

changes were observed in H, M and L cells compared to control cells (Figure 2b), suggesting that *TMPRSS2:ERG* fusion contributes to PCa initiation and/or progression in a different way. Accordingly, ectopic *TMPRSS2:ERG* expression significantly increased PC3c cell migration in a membrane-based assay system (Figure 2c), as well as its invasiveness in a Matrigel-based system (Figure 2d). Interestingly, among H, M and L cells, the enhancements of cell motility and invasiveness seemed to depend on *TMPRSS2:ERG* expression levels: compared to control cells, H cells showed the most significant induction of cell migration (3.5 fold) and invasion (7.5 fold); whereas M cell migration (1.7 fold) and invasion (3.4 fold) were higher than those of L cells (migration: 1.2 fold; invasion: 1.2 fold) (Figure 2c and 2d). These results provide *in vitro* evidence that *TMPRSS2:ERG* promotes, in a dose-dependent manner, PC3c cell migration and invasion, two crucial attributes of cancer cell metastasis.

Genome-wide expression analysis reveals potential TMPRSS2:ERG target genes and their associated cell motility and invasiveness functions.

To decipher the molecular mechanisms that underlie *TMPRSS2:ERG*-mediated PC3c cell migration and invasion enhancements, we investigated global gene expression changes in H, M and L cells using Agilent 44k Whole Human Genome Expression arrays. Compared to control cells, 1673 genes showed significant differential expression (adjusted P-value <0.01) in H cells (809 upregulated genes and 864 downregulated genes) (Figure 3a), and 446 genes were differentially expressed in M cells (267 upregulated genes and 179 downregulated genes), whereas only 191 genes with differential expression were identified in L cells (101 upregulated genes and 90 downregulated genes). Therefore, the quantity of deregulated genes identified in H, M and L cells also appeared to rely on *TMPRSS2:ERG* expression levels in PC3c cells.

A comparison of H, M and L cell transcriptomic profiles revealed that 126 genes were commonly deregulated in H, M and L cells (hereafter referred to as “common deregulated

genes"), including 64 common upregulated genes and 62 common downregulated genes (Figure 3b, Supplementary Table S2 and S3). In particular, about 50% of these 126 common deregulated genes showed high, moderate and low expression levels in *TMPRSS2:ERG*-expressing H, M, L cells, respectively (Figure 3b and Supplementary Table S2 and S3). The "dose-dependent" expression profile of these genes suggested that they could be direct target genes of TMPRSS2:ERG. Among these genes, we noted the striking upregulation of *PLAT (Tissue-type plasminogen activator)*, a well-known TMPRSS2:ERG target gene in PCa (4, 36, 37). Moreover, the over-expression of some of these genes has been shown to be associated with PCa progression and poor clinical outcomes, such as *CD44* (38), *MMP9* (39) and *FSCN1 (Fascin homolog 1)* (40). To understand the overall functional significance of these common 126 deregulated genes, we used the DAVID gene ontology analysis (41). Among the top Gene Ontology (GO) terms, we noted that "*cell motion*", "*cell migration*" and "*metalloendopeptidase activity*", were upregulated, whereas "*transcription*" and "*regulation of apoptosis*" were downregulated (Figure 3c). Taken together, these transcriptomic studies were in agreement with the observed enhancements of PC3c cell migration and invasion, and further highlighted the *TMPRSS2:ERG* role in the PCa cell metastasis process.

Turning to the identification of TMPRSS2:ERG direct target genes in PCa, we focused on two candidate target genes in the following studies. The first one was *MMP9*, also known as *Gelatinase B*, which has been shown to be associated with PCa progression (39), and also regulated by other ETS transcription factors in diverse types of cancer cells including PCa (42, 43). However, it was not clear whether TMPRSS2:ERG could directly regulate *MMP9* expression in PCa. The second potential target gene was *PLXNA2*, a type I trans-membrane glycoprotein that functions as a receptor for Semaphorins. Together with other Plexins, it was initially considered to mediate axon guidance during development (44). However, recent studies have revealed Semaphorin-Plexin signaling outside of the nervous system, providing

additional information about this signaling in cancer (45). For instance, *PLXNB1* (*Plexin B1*) gene mutations in human PCa samples have been shown to be associated with PCa cell motility and invasion enhancements (46). These findings, together with the phenotype observed in H, M and L cells, prompted us to further investigate whether TMPRSS2:ERG could directly control *MMP9* and *PLXNA2* expression to increase PCa cell migration and invasion.

MMP9 and PLXNA2 expression levels were associated with TMPRSS2:ERG expression in human PCa samples

To investigate whether *MMP9* and *PLXNA2* are genuine target genes of TMPRSS2:ERG in PCa, we first examined their expression in human PCa samples. We used RNA from a PCa cohort composed of 52 human prostatectomy specimens from the Tumor Tissue Bank, C2RC, Lille University Hospital (CHRU Lille) (Supplementary Table S4). Among these PCa samples, we found, using *TMPRSS2:ERG*-specific primers (4), 32 samples that showed detectable *TMPRSS2:ERG* fusion transcripts (61.5%). In this PCa cohort, *MMP9* and *PLXNA2* expression levels were significantly higher in *TMPRSS2:ERG*-positive PCa samples than in *TMPRSS2:ERG*-negative samples ($P=0.0055$ and $P<0.0001$ respectively) (Figures 4a and 4b).

To further examine the associations between *TMPRSS2:ERG* and its potential targets, *MMP9* and *PLXNA2*, we performed a two-tailed non-parametric Spearman correlation analysis. Given the heterogeneity of *TMPRSS2:ERG* transcripts detected in PCa samples (5, 34), it is difficult to design universal specific primers to accurately quantify total *TMPRSS2:ERG* expression. We therefore used *ERG*-specific primers that could detect not only *ERG* transcripts, but also *TMPRSS2:ERG* transcripts. Importantly, high *ERG* expression was detected only in *TMPRSS2:ERG*-positive PCa samples, whereas *ERG* expression in fusion negative PCa samples was very low (Supplementary Figure S2), suggesting that, in this PCa

cohort, high-level *ERG* transcripts may be a direct consequence of the presence of *TMPRSS2:ERG* fusion. Spearman correlation analysis showed that *MMP9* expression was significantly correlated with *ERG* expression (R=0.4287, P=0.0015) (Figure 4c), as was *PLXNA2* expression (R=0.6178, P<0.001) (Figure 4d). Thus, *MMP9* and *PLXNA2* expression levels were upregulated in *TMPRSS2:ERG*-positive PCa specimens, and their expression levels were correlated with *ERG* expression in PCa samples.

TMPRSS2:ERG directly and positively regulates MMP9 expression in PCa cells

To determine whether *MMP9* gene expression was directly controlled by TMPRSS2:ERG in PCa cells, we first performed a chromatin immunoprecipitation assay (ChIP) in H cells and control cells. By analyzing the promoter region of the *MMP9* gene, we found a putative ETS-binding site (EBS) within 1 kb from the *MMP9* transcription start site (TSS) (Figure 5a, top panel). ChIP assay showed significant binding of TMPRSS2:ERG on this EBS in H cells (Figure 5a, bottom panel), whereas no TMPRSS2:ERG binding was found on this EBS in control cells, or in the promoter region of *GAPDH* gene which does not contain any functional EBS, suggesting direct and specific TMPRSS2:ERG binding to the *MMP9* promoter region in PC3c cells.

Next, dose-dependent upregulation of *MMP9* gene expression was confirmed by RT-qPCR in H, M and L cells (Figure 5b). In addition, we found that ectopic expression of TMPRSS2:ERG in DU145 cells, another AR and fusion double-negative PCa cell model, also resulted in increased *MMP9* expression (Figure 5c and Supplementary Figure S3). Because it has been shown that secreted MMP9 has an important role in extracellular matrix remodeling during cancer progression (47), we further investigated secreted MMP9 levels in *TMPRSS2:ERG*-expressing cells using a gelatin zymography assay. As expected, compared to control cells, more secreted MMP9 was found in *TMPRSS2:ERG*-expressing H and M cell conditioned mediums (Figure 5d). In particular, the cell gelatin degradation assay highlighted

the association between increased MMP9 secretion and the enhancement of gelatin matrix degradation in *TMPRSS2:ERG*-expressing H cells (Figure 5e and Supplementary Figure S4). Moreover, the knockdown of *TMPRSS2:ERG* in H cells using pooled *ERG* siRNA (Supplementary Figure S5) led to over 40% reduction of *MMP9* expression (Figure 5f), as well as decreased MMP9 secretion (Figure 5g). Similar results were also observed in M cells (Supplementary Figure S6) as well as in *TMPRSS2:ERG*-expressing DU145 cells (Supplementary Figure S7). Taken together, these results indicate that TMPRSS2:ERG is capable to directly and positively regulate MMP9 in PCa cells.

PLXNA2 is directly and positively regulated by TMPRSS2:ERG in PCa cells

Plexin A2 (*PLXNA2*) is another candidate TMPRSS2:ERG target gene identified by our transcriptomic studies (Figure 3b), and its expression was found to be upregulated in *TMPRSS2:ERG*-positive PCa samples and correlated with *ERG* expression in PCa specimens. A putative EBS, located within 1 kb from the *PLXNA2* gene TSS, was found in the *PLXNA2* promoter region (Figure 6a, top panel). The ChIP assay showed significant TMPRSS2:ERG binding on this EBS in H cells, but not in control cells (Figure 6a, bottom panel). Moreover, this binding was absent in the irrelevant GAPDH promoter region, indicating TMPRSS2:ERG directly and specifically binds to the *PLXNA2* promoter in PC3c cells.

The dose-dependent increase of *PLXNA2* expression was then confirmed in *TMPRSS2:ERG*-expressing H, M and L cells compared to control cells (Figure 6b). In addition, *PLXNA2* upregulation was also observed in *TMPRSS2:ERG*-expressing DU145 cells (Figure 6c and Supplementary Figure S3). An immunofluoresence assay also showed PLXNA2 protein induction in *TMPRSS2:ERG*-expressing H cells (Figure 6e, left panel). Importantly, *TMPRSS2:ERG* knockdown in H cells resulted in about 50% reduction of *PLXNA2* mRNA levels (Figure 6d), as well as PLXNA2 protein immunostaining (Figure 6e, right panel). Similar results were observed in M cells (Supplementary Figure S6) and *TMPRSS2:ERG*-

expressing DU145 cells (Supplementary Figure S7). These results therefore highlight that TMPRSS2:ERG can directly and positively regulate PLXNA2 expression in PCa cells.

***PLXNA2, but not MMP9, contributes to TMPRSS2:ERG-induced PC3c cell migration and invasion* in vitro.**

To further explore whether MMP9 and PLXNA2 were direct mediators of *TMPRSS2:ERG*-induced pro-motility and pro-invasion phenotypes observed in PCa cells, we performed migration and invasion assays using H cells in which ERG, MMP9 and PLXNA2 were knocked down, respectively. The pooled *MMP9* siRNA efficiently knocked down *MMP9* expression (Supplementary Figure S8a) as well as MMP9 secretion in H cells (Supplementary Figure S8b). Efficient *PLXNA2* knockdown effects were as well observed using pooled *PLXNA2* siRNA in H cells (Figure 7a and 7b).

In H cells, *ERG* knockdown dramatically decreased cell migration by over 50% (Figure 7c), and cell invasion by 70% (Figure 7d), indicating that the inductions of cell migration and invasion are specific to ectopic *TMPRSS2:ERG* expression. Surprisingly, *MMP9* knockdown had no significant effect on cell migration or invasion in H cells (Supplementary Figure S8c and S8d), whereas *PLXNA2* knockdown in H cells resulted in a 30% decrease in cell migration (Figure 7c) and a 20% decrease in cell invasion (Figure 7d). Hence, these findings demonstrate that PLXNA2 upregulation, but not MMP9 upregulation, may contribute, at least in part, to *TMPRSS2:ERG*-mediated induction of PC3c cell migration and invasion *in vitro*.

Furthermore, increased cell motility and invasiveness are considered as attributes commonly acquired by PCa cells during metastatic progression (48). Whether PLXNA2 expression is associated with metastatic PCa remains unclear. We therefore analyzed *PLXNA2* expression in microarray datasets from three independent PCa cohorts (49-51). As shown in Figures 7e, 7f and 7g, compared to primary PCa samples, *PLXNA2* expression levels were significantly higher in the metastatic PCa, substantiating its potential role in PCa metastasis.

DISCUSSION

Although the presence of chromosomal abnormalities have commonly been observed in hematologic malignancies and sarcomas (52), it was only in 2005, using conceptually new bioinformatics approaches, that the first gene fusions were identified in a large proportion of PCa (4). While the gene fusions initially found in PCa were *ETS* transcription factors (*ERG* and *ETV1*) fused to the 5' part of the prostate-specific gene *TMPRSS2*, it is now clear that they may involve other *ETS* family members (i.e., *Fli-1*, *ELK4*), novel 5' partners and a class of non-ETS-based fusions (3). However, the *TMPRSS2:ERG* fusion remains the most prevalent chromosomal rearrangement in PCa (3). To date, this fusion has been identified not only in androgen-responsive PCa, but also in androgen-refractory PCa (16).

Here, using three AR-negative PC3c cell clones with different *TMPRSS2:ERG* expression levels, we demonstrated that ectopic expression of *TMPRSS2:ERG* can induce, in a dose-dependent manner, PC3c cell motility and invasiveness. These findings are in agreement with the role of the *TMPRSS2:ERG* fusion as revealed using various PCa cell models (4, 18, 21, 35, 53). Importantly, inhibition of endogenous *TMPRSS2:ERG* expression in AR-positive VCaP cells significantly reduced cell invasiveness (17, 18). Given the diverse genetic backgrounds of PCa cell models used in studies, the common function of *TMPRSS2:ERG* fusion is to improve PCa cell motility and invasiveness. Furthermore, since *TMPRSS2:ERG*-induced cell migration and invasion have been shown in AR-positive and -negative PCa cells, this function does not seem to be associated with the AR status of PCa cells. Increased cell motility and invasiveness are the essential hallmarks of cancer, as well as prerequisites for local tumor progression and metastasis (48). Interestingly, recent clinical studies also revealed the presence of *TMPRSS2:ERG* fusion in circulating tumor cells isolated from PCa patients with metastatic disease and in castration-resistant PCa patients (54, 55). In addition, *TMPRSS2:ERG*-positive foci in multifocal PCa have a greater predilection for lymph node

metastasis (56, 57). These clinical findings highlight the potential role of TMPRSS2:ERG in PCa metastasis.

Increased cell motility and invasiveness are also associated with cells adopting a mesenchymal phenotype (58). The epithelial-to-mesenchymal transition (EMT) is considered to be one of key steps for cells to acquire metastatic adaptation (59). Three previous studies have also demonstrated that EMT is one of the consequences of *TMPRSS2:ERG* expression in PCa cell models (37, 53, 60). Accordingly, PC3c cells with high *TMPRSS2:ERG* expression (H cells) demonstrated a more elongated and scattered mesenchymal morphology. However, the absence of differential expression of EMT markers, such as *E-Cadherin, Vimentin*, *Twist1* and *Snail* in our cell models (Supplementary Figure S9), raised two questions that need to be addressed in future studies: 1) Among our cell models (H, M and L cells), the highest *TMPRSS2:ERG* expression was only 50% of that found in VCaP cells; is there a threshold of ERG expression necessary to induce EMT in PCa cells? 2) Is *TMPRSS2:ERG*-induced EMT independent of AR signaling?

MMP9 expression has been shown to be correlated with increased invasive and metastatic phenotypes in various tumor types including prostate cancer (39, 61, 62). Here, we showed that MMP9 was positively and directly regulated by TMPRSS2:ERG in PC3c cells and its expression was correlated with *ERG* expression in PCa samples. In fact, several transcription factors, such as NF-κB, SP-1, AP-1 and ETS have been shown to control MMP9 expression in physiological and pathological conditions (63-65). Although it has been reported that ETS-1 promotes the invasiveness of paclitaxel-resistant and hormone-refractory PCa cells by increasing MMP9 expression (66), a recent study reported that SPDEF, another ETS transcription factor, suppresses prostate cancer cell invasion through the repression of MMP9 expression (42). Together with our results, these findings highlight the importance of the functional specificity of ETS transcription factors in controlling MMP9 expression in PCa.

Furthermore, although increased secretion of MMP9 and corresponding gelatin matrix degradation were observed in our cell model, *MMP9* knockdown did not impair TMPRSS2:ERG-induced cell migration or invasion in the membrane-based transwell assays. Similar results have also been observed in *TMPRSS2:ERG* or *ERG*-expressing RWPE-1 and BPH-1 cells treated with the pan-MMP inhibitor or a MMP2/9 specific inhibitor (4, 18), suggesting that, under membrane-based transwell assay systems, increased MMP9 expression is not essential for TMPRSS2:ERG-induced cell migration and invasion. Of particular interest, MMP9 has been shown to trigger the release of the matrix-bound VEGF, thus promoting tumor angiogenesis (67), and remodeling the pro-metastatic microenvironment of the metastatic niche (47, 68). Therefore, future studies are required to determine the role of MMP9 in *TMPRSS2:ERG*-positive PCa cells using *in vivo* models.

Plexin receptors and their Semaphorin ligands were initially identified as evolutionarily conserved axon-guidance cues in the nervous system (69). However, increasing evidence highlights their role outside the nervous system, and particularly in cancer metastasis and progression (45). In particular, there is supporting evidence that somatic aberrations of Plexins and Semaphorins are involved in pancreatic carcinogenesis (70). Although their functions are poorly understood in PCa, Plexin receptors and its Semaphorin ligands have been shown to be expressed in diverse PCa cell lines and tissues (71). The overexpression of *PLXNB1* with somatic missense mutations is functionally associated with increased PCa cell motility and invasiveness, as well as disease metastatic progression (46, 72). We showed in the present study that that TMPRSS2:ERG positively and directly regulates PLXNA2 expression in PC3c cells. Interestingly, during mouse (73, 74) and chicken development (75, 76), the *Erg* expression profile overlaps with that of *Plxna2* in migrating neural crest cells and aorta, suggesting the possible direct regulation of Plxna2 by the Erg transcription factor in development process. Moreover, other transcription factors may also control PLXNA2

expression. For example, GATA6 has been shown to directly regulate PLXNA2 expression during human cardiac outflow tract development (77). Furthermore, the pleiotropic signals mediated by Semaphorin-Plexin have been shown to positively or negatively control multiple functions in tumor cells, including their migration and invasion abilities (45). We showed that the upregulation of PLXNA2 contributes, at least in part, to *TMPRSS2:ERG*-induced PC3c cell migration and invasion. In agreement with these findings *in vitro*, analysis of microarray datasets provided evidence that *PLXNA2* expression is up-regulated in metastatic PCa, supporting the potential involvement of PLXNA2 in PCa metastatic spread.

In summary, using an AR-negative PCa model, we confirmed the important role of *TMPRSS2:ERG* in PCa cell migration and invasion, and identified two "cell motility"- and "invasiveness"-related direct target genes, *MMP9* and *PLXNA2,* providing novel insights into the role of *TMPRSS2:ERG* in PCa metastasis.

MATERIALS AND METHODS

Cell culture and Chemical reagents

PC3c cells (32) and DU145 cells (ATCC) were cultured in DMEM supplemented with 10% fetal bovine serum and sub-cultured every 3-4 days. Unless otherwise stated, all chemical reagents were from Sigma-Aldrich.

Generation of plasmids and retrovirus constructs

The *TMPRSS2:ERG* cDNA was isolated from a fusion-positive PCa patient sample, and sub-cloned into a pcDNA3.1(+) (Invitrogen) or retrovirus pLPCX vector (Clontech). The primers used for cloning are listed in Supplementary Table S1. Amplified plasmids were purified on NucleoBond Xtra Midi endotoxin-free columns (Macherey-Nagel) and sequenced prior to use.

Generation of TMPRSS2:ERG-expressing cells

Low passage PC3c cells were transfected with a *TMPRSS2:ERG* expression vector or empty pcDNA vector using FuGENE® 6 Reagent (Roche) according to the manufacturer's instruction, then selected in routine culture medium containing 400 mg/mL G418 antibiotic (Life Technologies) for 3 weeks. The pLPCX- or pLPCX/TMPRSS2:ERG-containing retroviruses were transduced into DU145 cells to generate *TMPRSS2:ERG*-expressing cells according to the manufacturer's instructions (Clontech).

Short interfering RNAs (siRNA) transfection

Pre-designed pooled siRNA were obtained from Dharmaco-Termo Scientific. Cells were transfected with the siRNA (50 nM) using Lipofectamine 2000 reagent (Invitrogen) according to the manufacturer's instructions. Gene knockdown effects were evaluated after 72 h of transfection. The siRNA used in this study were siERG (ON-TARGETplus SMARTpool L-003886-00), siMMP9 (ON-TARGETplus SMARTpool L-005970-00), siPLXNA2 (ON-TARGETplus SMARTpool L-021532-01) and the control siRNA (ON-TARGETplus Non-targeting Pool D-001810-10).

Protein extraction and immunoblotting

Proteins were extracted and immunoblotted (Western Blotting) as described previously (78). Antibodies used in immunoblotting were: rabbit monoclonal anti-ERG (Epitomics 2085, dilution 1:1 000), mouse monoclonal anti β-ACTIN (Sigma Clone AC-15, dilution 1:10 000), rabbit polyclonal anti HPRT (Santa Cruz sc-20975, dilution 1:1 000), Rabbit IgG-HRP (GE Healthcare NA934V, dilution 1:10 000) and Mouse IgG-HRP (Santa Cruz, 1:10 000).

Cell proliferation, migration and invasion assay

Cell proliferation assays were performed in quadruplicate using CellTiter-Glo® kit (Promega) in 96-well plate (2 500 cells/well) according to the manufacturer's recommendations, and luminescence was measured using a Centro LB 960 microplate luminometer (Berthold) at indicated times.

Cell migration assays and cell invasion assays were performed with 100 000 cells in triplicate using a FluoroBlok™ 8 µm pores 24-well insert system (BD Biosciences) and 24-well BioCoat™ Tumor Invasion System (BD Biosciences) according to the manufacturer's instructions. After 16 h of incubation, cells were labeled with 10 µg/mL $DilC_{12}(3)$ fluorescent dye (BD Biosciences), and the migrated or invaded cells were measured using a FLUOstar OPTIMA lecturer (BMG Labtech).

Gelatin degradation assay and gelatin zymography analysis

Gelatin degradation assay was performed as described previously (79). To perform the gelatin zymography assay, cells were rinsed and incubated with medium without FBS for 24 h. Then the conditioned mediums (CM) were collected, and total protein concentrations were measured and used to adjust loading quantity of CM. Equal amount of CMs were mixed with non-denaturing Laemmli blue loading dye, then loaded on a 7% SDS-PAGE gel containing 0.1% (w/v) gelatin. After migration, the gel was incubated with zymogram renaturing buffer and zymogram developing buffer. Finally, the gel was stained with 0.5% (w/v) Coomassie

Blue R-250 and destained with a solution containing 40% (v/v) ethanol and 10% (v/v) acetic acid.

Cell total RNA preparation and RT-qPCR

Cell total RNA was purified using the NucleoSpin® RNA II kit (Macherey Nagel) according to the manufacturer's instructions. Then, 1 µg total RNA was used to generate cDNA strand using the High Capacity RNA-to-cDNA kit (Applied Biosystems). Quantitative polymerase chain reactions (qPCRs) were performed using the Power SYBR Green PCR Master kit (Applied Biosystems) on a Stratagene Mx3005P qPCR System according to manufacturer's instructions. Individual gene relative expression level was calculated using the $2^{-\Delta\Delta CT}$ method and normalized to that of the housekeeping gene *18S*. Optimal primer specificity and efficiency were validated according to the Mx3005P qPCR System user's guide. The primers used in this study can be found in Supplementary Table S1.

Immunofluorescence

Immunofluorescence (IF) assays were performed as described (78). The antibodies used in this study were monoclonal rabbit anti-ERG (Epitomics 2805, dilution 1:200), monoclonal rat anti-PLXNA2 (R&D Systems, MAB5486, 10 µg/mL), Alexa Fluo®-488 conjugated anti-rabbit IgG (Invitrogen, dilution 1:500) and Alexa Fluo®-555 anti-rat IgG (Invitrogen, dilution 1:500). Images were acquired using an LSM 710 confocal microscopy system and ZEN 2010 software (Carl Zeiss).

Microarray analysis

Microarray analyses were conducted following the Two-Color Microarray-Based Expression Analysis Protocol (Agilent Technologies). For each sample, 1 µg of total RNA was divided into two equal aliquots to enable technical replication known as "dye-swap hybridization". The reverse transcription and the labeling procedure were performed using the protocol recommended by Agilent Technologies (Low RNA Input Fluorescent Linear Amplification

Kit). Hybridizations were performed on Agilent Whole Human Genome 44K microarrays for 17 hours at 65°C using the Agilent Gene Expression Hybridization kit. Arrays were washed and scanned using Innoscan 700 (Innopsys) and the raw data were processed and normalized using the Limma package (Linear Models for Microarray Data) running under the R environment. Gene Ontology analysis was performed using the DAVID program as described (41).

Chromatin immunoprecipitation (ChIP)

ChIP assay was performed as described (80). Antibodies used were polyclonal rabbit anti ERG antibody (Santa Cruz sc-353) or control rabbit IgG antibody (Santa Cruz). The genomic DNA was purified using NucleoSpin® Clean-up columns (Macherey-Nagel) according to protocol recommended by the manufacturer. Immunopreciptated genomic DNA was analyzed by PCR and details of the primers used can be found in Supplementary Table S1.

Human PCa samples

Human PCa samples (n=52) were obtained from the local tumor tissue bank, C2RC (Lille, France) after approval by the internal review board (CSTMT-042, 27/07/2009). Sampled and subsequently frozen tumor tissues originated from radical prostatectomies or trans-urethral prostatic resections performed at Lille University Hospitals (CHRU de Lille). All patients were informed and consent was obtained by the referring physician. To extract RNA, tissue samples were first homogenized in TRIzol® (Invitrogen), and total RNA was prepared using NucleoSpin® RNA II columns (Macherey-Nagel). The RNA quality and quantity were accessed by the Agilent 2100 Bioanalyser system. Pathological findings of these PCa samples can be found in Supplementary Table S4.

Image treatment and Statistical analysis

All images treatments were carried out using Image J or Photoshop CS software. Statistical analysis was performed using GraphPad Prism software. Statistical methods used in this study

are indicated in the corresponding figure legends. Unless otherwise indicated, all values in the figures are expressed as means ± SEM.

CONFLICT OF INTEREST

The authors declare no conflict of interest.

ACKNOWLEDGEMENTS

The authors would like to thank A. Fradet, M. Le Jeune, M. Holder, C. Delliaux, G. Boulay, M. Dubuissez, I. Loison, Z. Kherrouche and N. Malaquin and for their excellent technical advices; D. Lacorre, E. Werkmeister from the BioImaging Center Lille Nord de France for their technical assistance; E. Lelièvre and D. Leprince for their stimulating discussions; C. Engel-Gautier for her critical reading of the manuscript. The authors thank the local Tumor Tissue Bank (Tumorothèque), Regional Reference Oncology Center (CRRC) (Head, Pr. M.C. Copin) in Lille, France. This work was supported by grants from the *Centre national de la recherche scientifique* (CNRS), *La Ligue contre le Cancer* (Comité du Pas-de-Calais) and the *Institut national du cancer* (INCa_4419). T.V. Tian is a recipient of Ph.D. fellowships from the Institut Pasteur of Lille/Nord-Pas-de-Calais Regional Council (Région Nord-Pas-de Calais) and the *Association pour la recherche sur le cancer* (ARC).

REFERENCES

1. Siegel R, Naishadham D, Jemal A. Cancer statistics, 2012. CA Cancer J Clin. 2012 Jan-Feb;62(1):10-29.

2. Squire JA, Park PC, Yoshimoto M, Alami J, Williams JL, Evans A, et al. Prostate cancer as a model system for genetic diversity in tumors. Adv Cancer Res. 2011;112:183-216.

3. Rubin MA, Maher CA, Chinnaiyan AM. Common gene rearrangements in prostate cancer. J Clin Oncol. 2011 Sep 20;29(27):3659-68.

4. Tomlins SA, Rhodes DR, Perner S, Dhanasekaran SM, Mehra R, Sun XW, et al. Recurrent fusion of TMPRSS2 and ETS transcription factor genes in prostate cancer. Science. 2005 Oct 28;310(5748):644-8.

5. Wang J, Cai Y, Ren C, Ittmann M. Expression of variant TMPRSS2/ERG fusion messenger RNAs is associated with aggressive prostate cancer. Cancer Res. 2006 Sep 1;66(17):8347-51.

6. FitzGerald LM, Agalliu I, Johnson K, Miller MA, Kwon EM, Hurtado-Coll A, et al. Association of TMPRSS2-ERG gene fusion with clinical characteristics and outcomes: results from a population-based study of prostate cancer. BMC Cancer. 2008;8:230.

7. Gopalan A, Leversha MA, Satagopan JM, Zhou Q, Al-Ahmadie HA, Fine SW, et al. TMPRSS2-ERG gene fusion is not associated with outcome in patients treated by prostatectomy. Cancer Res. 2009 Feb 15;69(4):1400-6.

8. Hoogland AM, Jenster G, van Weerden WM, Trapman J, van der Kwast T, Roobol MJ, et al. ERG immunohistochemistry is not predictive for PSA recurrence, local recurrence or overall survival after radical prostatectomy for prostate cancer. Modern pathology : an official journal of the United States and Canadian Academy of Pathology, Inc. 2012 Mar;25(3):471-9.

9. Hermans KG, Boormans JL, Gasi D, van Leenders GJ, Jenster G, Verhagen PC, et al. Overexpression of prostate-specific TMPRSS2(exon 0)-ERG fusion transcripts corresponds with favorable prognosis of prostate cancer. Clinical cancer research : an official journal of the American Association for Cancer Research. 2009 Oct 15;15(20):6398-403.

10. Saramaki OR, Harjula AE, Martikainen PM, Vessella RL, Tammela TL, Visakorpi T. TMPRSS2:ERG fusion identifies a subgroup of prostate cancers with a favorable prognosis. Clinical

cancer research : an official journal of the American Association for Cancer Research. 2008 Jun 1;14(11):3395-400.

11. Attard G, Clark J, Ambroisine L, Fisher G, Kovacs G, Flohr P, et al. Duplication of the fusion of TMPRSS2 to ERG sequences identifies fatal human prostate cancer. Oncogene. 2008 Jan 10;27(3):253-63.

12. Demichelis F, Fall K, Perner S, Andren O, Schmidt F, Setlur SR, et al. TMPRSS2:ERG gene fusion associated with lethal prostate cancer in a watchful waiting cohort. Oncogene. 2007 Jul 5;26(31):4596-9.

13. Nam RK, Sugar L, Wang Z, Yang W, Kitching R, Klotz LH, et al. Expression of TMPRSS2:ERG gene fusion in prostate cancer cells is an important prognostic factor for cancer progression. Cancer Biol Ther. 2007 Jan;6(1):40-5.

14. Nam RK, Sugar L, Yang W, Srivastava S, Klotz LH, Yang LY, et al. Expression of the TMPRSS2:ERG fusion gene predicts cancer recurrence after surgery for localised prostate cancer. British journal of cancer. 2007 Dec 17;97(12):1690-5.

15. Perner S, Demichelis F, Beroukhim R, Schmidt FH, Mosquera JM, Setlur S, et al. TMPRSS2:ERG fusion-associated deletions provide insight into the heterogeneity of prostate cancer. Cancer Res. 2006 Sep 1;66(17):8337-41.

16. Mehra R, Tomlins SA, Yu J, Cao X, Wang L, Menon A, et al. Characterization of TMPRSS2-ETS gene aberrations in androgen-independent metastatic prostate cancer. Cancer Res. 2008 May 15;68(10):3584-90.

17. Tomlins SA, Laxman B, Varambally S, Cao X, Yu J, Helgeson BE, et al. Role of the TMPRSS2-ERG gene fusion in prostate cancer. Neoplasia. 2008 Feb;10(2):177-88.

18. Klezovitch O, Risk M, Coleman I, Lucas JM, Null M, True LD, et al. A causal role for ERG in neoplastic transformation of prostate epithelium. Proc Natl Acad Sci U S A. 2008 Feb 12;105(6):2105-10.

19. Zong Y, Xin L, Goldstein AS, Lawson DA, Teitell MA, Witte ON. ETS family transcription factors collaborate with alternative signaling pathways to induce carcinoma from adult murine prostate cells. Proc Natl Acad Sci U S A. 2009 Jul 28;106(30):12465-70.

20. King JC, Xu J, Wongvipat J, Hieronymus H, Carver BS, Leung DH, et al. Cooperativity of TMPRSS2-ERG with PI3-kinase pathway activation in prostate oncogenesis. Nature genetics. 2009 May;41(5):524-6.

21. Carver BS, Tran J, Gopalan A, Chen Z, Shaikh S, Carracedo A, et al. Aberrant ERG expression cooperates with loss of PTEN to promote cancer progression in the prostate. Nature genetics. 2009 May;41(5):619-24.

22. Yu J, Yu J, Mani RS, Cao Q, Brenner CJ, Cao X, et al. An integrated network of androgen receptor, polycomb, and TMPRSS2-ERG gene fusions in prostate cancer progression. Cancer Cell. 2010 May 18;17(5):443-54.

23. Wei GH, Badis G, Berger MF, Kivioja T, Palin K, Enge M, et al. Genome-wide analysis of ETS-family DNA-binding in vitro and in vivo. Embo J. 2010 Jul 7;29(13):2147-60.

24. Chng KR, Chang CW, Tan SK, Yang C, Hong SZ, Sng NY, et al. A transcriptional repressor co-regulatory network governing androgen response in prostate cancers. Embo J. 2011 Jun 13;31(12):2810-23.

25. Macintosh CA, Stower M, Reid N, Maitland NJ. Precise microdissection of human prostate cancers reveals genotypic heterogeneity. Cancer Res. 1998 Jan 1;58(1):23-8.

26. Cheng L, Song SY, Pretlow TG, Abdul-Karim FW, Kung HJ, Dawson DV, et al. Evidence of independent origin of multiple tumors from patients with prostate cancer. J Natl Cancer Inst. 1998 Feb 4;90(3):233-7.

27. Andreoiu M, Cheng L. Multifocal prostate cancer: biologic, prognostic, and therapeutic implications. Hum Pathol. 2010 Jun;41(6):781-93.

28. Mehra R, Han B, Tomlins SA, Wang L, Menon A, Wasco MJ, et al. Heterogeneity of TMPRSS2 gene rearrangements in multifocal prostate adenocarcinoma: molecular evidence for an independent group of diseases. Cancer Res. 2007 Sep 1;67(17):7991-5.

29. Barry M, Perner S, Demichelis F, Rubin MA. TMPRSS2-ERG fusion heterogeneity in multifocal prostate cancer: clinical and biologic implications. Urology. 2007 Oct;70(4):630-3.

30. Minner S, Gartner M, Freudenthaler F, Bauer M, Kluth M, Salomon G, et al. Marked heterogeneity of ERG expression in large primary prostate cancers. Modern pathology : an official journal of the United States and Canadian Academy of Pathology, Inc. 2012 Aug 17.

31. Furusato B, Tan SH, Young D, Dobi A, Sun C, Mohamed AA, et al. ERG oncoprotein expression in prostate cancer: clonal progression of ERG-positive tumor cells and potential for ERG-based stratification. Prostate Cancer Prostatic Dis. 2010 Sep;13(3):228-37.

32. Fradet A, Sorel H, Deux B, Clézardin P, Bonnelye E. A new murine model of osteoblastic/osteolytic lesions from human androgen-resistant prostate cancer. Bone. 2010;47(Special Issue):S289.

33. Scher HI, Morris MJ, Basch E, Heller G. End points and outcomes in castration-resistant prostate cancer: from clinical trials to clinical practice. J Clin Oncol. 2011 Sep 20;29(27):3695-704.

34. Clark J, Merson S, Jhavar S, Flohr P, Edwards S, Foster CS, et al. Diversity of TMPRSS2-ERG fusion transcripts in the human prostate. Oncogene. 2007 Apr 19;26(18):2667-73.

35. Wang J, Cai Y, Yu W, Ren C, Spencer DM, Ittmann M. Pleiotropic biological activities of alternatively spliced TMPRSS2/ERG fusion gene transcripts. Cancer Res. 2008 Oct 15;68(20):8516-24.

36. Kunderfranco P, Mello-Grand M, Cangemi R, Pellini S, Mensah A, Albertini V, et al. ETS transcription factors control transcription of EZH2 and epigenetic silencing of the tumor suppressor gene Nkx3.1 in prostate cancer. PLoS One. 2010;5(5):e10547.

37. Gupta S, Iljin K, Sara H, Mpindi JP, Mirtti T, Vainio P, et al. FZD4 as a mediator of ERG oncogene-induced WNT signaling and epithelial-to-mesenchymal transition in human prostate cancer cells. Cancer Res. 2010 Sep 1;70(17):6735-45.

38. Patrawala L, Calhoun T, Schneider-Broussard R, Li H, Bhatia B, Tang S, et al. Highly purified CD44+ prostate cancer cells from xenograft human tumors are enriched in tumorigenic and metastatic progenitor cells. Oncogene. 2006 Mar 16;25(12):1696-708.

39. Castellano G, Malaponte G, Mazzarino MC, Figini M, Marchese F, Gangemi P, et al. Activation of the osteopontin/matrix metalloproteinase-9 pathway correlates with prostate cancer

progression. Clinical cancer research : an official journal of the American Association for Cancer Research. 2008 Nov 15;14(22):7470-80.

40. Nese N, Kandiloglu AR, Simsek G, Lekili M, Ozdamar A, Catalkaya A, et al. Comparison of the desmoplastic reaction and invading ability in invasive ductal carcinoma of the breast and prostatic adenocarcinoma based on the expression of heat shock protein 47 and fascin. Anal Quant Cytol Histol. 2010 Apr;32(2):90-101.

41. Huang da W, Sherman BT, Lempicki RA. Systematic and integrative analysis of large gene lists using DAVID bioinformatics resources. Nat Protoc. 2009;4(1):44-57.

42. Steffan JJ, Koul S, Meacham RB, Koul HK. The Transcription Factor SPDEF Suppresses Prostate Tumor Metastasis. J Biol Chem. 2012 Aug 24;287(35):29968-78.

43. Himelstein BP, Lee EJ, Sato H, Seiki M, Muschel RJ. Transcriptional activation of the matrix metalloproteinase-9 gene in an H-ras and v-myc transformed rat embryo cell line. Oncogene. 1997 Apr 24;14(16):1995-8.

44. Franco M, Tamagnone L. Tyrosine phosphorylation in semaphorin signalling: shifting into overdrive. EMBO Rep. 2008 Sep;9(9):865-71.

45. Capparuccia L, Tamagnone L. Semaphorin signaling in cancer cells and in cells of the tumor microenvironment--two sides of a coin. J Cell Sci. 2009 Jun 1;122(Pt 11):1723-36.

46. Wong OG, Nitkunan T, Oinuma I, Zhou C, Blanc V, Brown RS, et al. Plexin-B1 mutations in prostate cancer. Proc Natl Acad Sci U S A. 2007 Nov 27;104(48):19040-5.

47. Deryugina EI, Quigley JP. Matrix metalloproteinases and tumor metastasis. Cancer Metastasis Rev. 2006 Mar;25(1):9-34.

48. Hanahan D, Weinberg RA. Hallmarks of cancer: the next generation. Cell. 2011 Mar 4;144(5):646-74.

49. Dhanasekaran SM, Barrette TR, Ghosh D, Shah R, Varambally S, Kurachi K, et al. Delineation of prognostic biomarkers in prostate cancer. Nature. 2001 Aug 23;412(6849):822-6.

50. Grasso CS, Wu YM, Robinson DR, Cao X, Dhanasekaran SM, Khan AP, et al. The mutational landscape of lethal castration-resistant prostate cancer. Nature. 2012 Jul 12;487(7406):239-43.

51. Varambally S, Yu J, Laxman B, Rhodes DR, Mehra R, Tomlins SA, et al. Integrative genomic and proteomic analysis of prostate cancer reveals signatures of metastatic progression. Cancer Cell. 2005 Nov;8(5):393-406.

52. Mitelman F, Johansson B, Mertens F. The impact of translocations and gene fusions on cancer causation. Nat Rev Cancer. 2007 Apr;7(4):233-45.

53. Leshem O, Madar S, Kogan-Sakin I, Kamer I, Goldstein I, Brosh R, et al. TMPRSS2/ERG promotes epithelial to mesenchymal transition through the ZEB1/ZEB2 axis in a prostate cancer model. PLoS One. 2011;6(7):e21650.

54. Attard G, Swennenhuis JF, Olmos D, Reid AH, Vickers E, A'Hern R, et al. Characterization of ERG, AR and PTEN gene status in circulating tumor cells from patients with castration-resistant prostate cancer. Cancer Res. 2009 Apr 1;69(7):2912-8.

55. Stott SL, Lee RJ, Nagrath S, Yu M, Miyamoto DT, Ulkus L, et al. Isolation and characterization of circulating tumor cells from patients with localized and metastatic prostate cancer. Sci Transl Med. 2010 Mar 31;2(25):25ra3.

56. Guo CC, Wang Y, Xiao L, Troncoso P, Czerniak BA. The relationship of TMPRSS2-ERG gene fusion between primary and metastatic prostate cancers. Hum Pathol. 2012 May;43(5):644-9.

57. Perner S, Svensson MA, Hossain RR, Day JR, Groskopf J, Slaughter RC, et al. ERG rearrangement metastasis patterns in locally advanced prostate cancer. Urology. 2010 Apr;75(4):762-7.

58. Polyak K, Weinberg RA. Transitions between epithelial and mesenchymal states: acquisition of malignant and stem cell traits. Nat Rev Cancer. 2009 Apr;9(4):265-73.

59. Valastyan S, Weinberg RA. Tumor metastasis: molecular insights and evolving paradigms. Cell. 2012 Oct 14;147(2):275-92.

60. Becker-Santos DD, Guo Y, Ghaffari M, Vickers ED, Lehman M, Altamirano-Dimas M, et al. Integrin-linked kinase as a target for ERG-mediated invasive properties in prostate cancer models. Carcinogenesis. 2012 Dec;33(12):2558-67.

61. Kessenbrock K, Plaks V, Werb Z. Matrix metalloproteinases: regulators of the tumor microenvironment. Cell. 2010 Apr 2;141(1):52-67.

62. Dos Reis ST, Pontes J, Jr., Villanova FE, Borra PM, Antunes AA, Dall'oglio MF, et al. Genetic polymorphisms of matrix metalloproteinases: susceptibility and prognostic implications for prostate cancer. J Urol. 2009 May;181(5):2320-5.

63. Nakamura Y, Esnault S, Maeda T, Kelly EA, Malter JS, Jarjour NN. Ets-1 regulates TNF-alpha-induced matrix metalloproteinase-9 and tenascin expression in primary bronchial fibroblasts. J Immunol. 2004 Feb 1;172(3):1945-52.

64. Hanzawa M, Shindoh M, Higashino F, Yasuda M, Inoue N, Hida K, et al. Hepatocyte growth factor upregulates E1AF that induces oral squamous cell carcinoma cell invasion by activating matrix metalloproteinase genes. Carcinogenesis. 2000 Jun;21(6):1079-85.

65. Hance MW, Dole K, Gopal U, Bohonowych JE, Jezierska-Drutel A, Neumann CA, et al. Secreted Hsp90 is a novel regulator of the epithelial to mesenchymal transition (EMT) in prostate cancer. J Biol Chem. 2012 Sep 18.

66. Kato T, Fujita Y, Nakane K, Kojima T, Nozawa Y, Deguchi T, et al. ETS1 promotes chemoresistance and invasion of paclitaxel-resistant, hormone-refractory PC3 prostate cancer cells by up-regulating MDR1 and MMP9 expression. Biochem Biophys Res Commun. 2012 Jan 20;417(3):966-71.

67. Bergers G, Brekken R, McMahon G, Vu TH, Itoh T, Tamaki K, et al. Matrix metalloproteinase-9 triggers the angiogenic switch during carcinogenesis. Nat Cell Biol. 2000 Oct;2(10):737-44.

68. Hiratsuka S, Nakamura K, Iwai S, Murakami M, Itoh T, Kijima H, et al. MMP9 induction by vascular endothelial growth factor receptor-1 is involved in lung-specific metastasis. Cancer Cell. 2002 Oct;2(4):289-300.

69. Kolodkin AL, Matthes DJ, Goodman CS. The semaphorin genes encode a family of transmembrane and secreted growth cone guidance molecules. Cell. 1993 Dec 31;75(7):1389-99.

70. Biankin AV, Waddell N, Kassahn KS, Gingras MC, Muthuswamy LB, Johns AL, et al. Pancreatic cancer genomes reveal aberrations in axon guidance pathway genes. Nature. 2012 Nov 15;491(7424):399-405.

71. Blanc V, Nariculam J, Munson P, Freeman A, Klocker H, Masters J, et al. A role for class 3 semaphorins in prostate cancer. Prostate. 2011 May;71(6):649-58.

72. Zhou C, Wong OG, Masters JR, Williamson M. Effect of cancer-associated mutations in the PlexinB1 gene. Mol Cancer. 2012;11:11.

73. Vlaeminck-Guillem V, Carrere S, Dewitte F, Stehelin D, Desbiens X, Duterque-Coquillaud M. The Ets family member Erg gene is expressed in mesodermal tissues and neural crests at fundamental steps during mouse embryogenesis. Mech Dev. 2000 Mar 1;91(1-2):331-5.

74. Brown CB, Feiner L, Lu MM, Li J, Ma X, Webber AL, et al. PlexinA2 and semaphorin signaling during cardiac neural crest development. Development. 2001 Aug;128(16):3071-80.

75. Toyofuku T, Yoshida J, Sugimoto T, Yamamoto M, Makino N, Takamatsu H, et al. Repulsive and attractive semaphorins cooperate to direct the navigation of cardiac neural crest cells. Dev Biol. 2008 Sep 1;321(1):251-62.

76. Dhordain P, Dewitte F, Desbiens X, Stehelin D, Duterque-Coquillaud M. Mesodermal expression of the chicken erg gene associated with precartilaginous condensation and cartilage differentiation. Mech Dev. 1995 Mar;50(1):17-28.

77. Kodo K, Nishizawa T, Furutani M, Arai S, Yamamura E, Joo K, et al. GATA6 mutations cause human cardiac outflow tract defects by disrupting semaphorin-plexin signaling. Proc Natl Acad Sci U S A. 2009 Aug 18;106(33):13933-8.

78. Le Jeune M, Tomavo N, Tian TV, Flourens A, Marchand N, Camuzeaux B, et al. Identification of four alternatively spliced transcripts of the Ucma/GRP gene, encoding a new Gla-containing protein. Exp Cell Res. 2010 Jan 15;316(2):203-15.

79. Sakurai-Yageta M, Recchi C, Le Dez G, Sibarita JB, Daviet L, Camonis J, et al. The interaction of IQGAP1 with the exocyst complex is required for tumor cell invasion downstream of Cdc42 and RhoA. J Cell Biol. 2008 Jun 16;181(6):985-98.

80. Flajollet S, Poras I, Carosella ED, Moreau P. RREB-1 is a transcriptional repressor of HLA-G. J Immunol. 2009 Dec 1;183(11):6948-59.

FIGURE LEGENDS

Figure 1 Stable ectopic expression of the *TMPRSS2:ERG* gene fusion in PC3c cells. (**a**) Schematic illustration of the *TMPRSS2:ERG* gene fusion expression plasmid construction. (**b**) Relative *ERG* expression was evaluated using qPCR in three *TMPRSS2:ERG*-expressing PC3c clone cells (H: PC3c cells with high *ERG* expression, M: PC3c cells with medium *ERG* expression and L: PC3c cells with low *ERG* expression), in control pcDNA clone cells, in HUVEC cells, as well as in VCaP cells. The expression levels of *ERG* in VCaP cells were normalized to 1. Results were obtained from three independent triplicate experiments. (**c**) Detection of TMPRSS2:ERG protein products (N-terminal-truncated ERG protein < 55 kDa) in H, M, L cells, control cells and parental PC3c cells. Total cell lysates were analyzed using Western blotting with ERG antibody, and human HPRT immunoblotting was used as a loading control.

Figure 2 Phenotype characterization of PC3c cells with ectopic TMPRSS2:ERG expression. (**a**) Phase contrast micrographs of H, M, L cells and control cells. Scale bar, 50 μm. (**b**) Cell proliferation assays were performed using the CellTiter-Glo kit (Promega) in quadruplicate for 5 days. Three independent experiments were performed and results are presented as relative luminescence unit (RLU) fold change compared to the RLU measured on Day 0. (**c**) Cell migration assays were performed using the FluoroBlok™ 8 μm pore 24-well insert system (BD Biosciences) in triplicate according to the manufacture's recommendations. Results are presented as relative fluorescence unit (RFU) fold change compared to control cells after 16 h. ****P<0.001*, **P<0.05*, one-way analysis of variance (ANOVA) with Dunnett's multiple comparison test. (**d**) Cell invasion assays were performed in triplicate using the 8 μm pore 24-well BioCoat™ Tumor Invasion system (BD Biosciences) according to the manufacturer's instructions. Results are presented as RFU fold change

compared to control cells measured after 16 hours. ***$P<0.001$, one-way analysis of variance (ANOVA) with Dunnett's multiple comparison test.

Figure 3 Transcriptomic studies of PC3c H, M and L cells. (**a**) Red Venn diagram shows 809 genes, 267 genes and 101 genes are upregulated in *TMPRSS2:ERG*-expressing H, M and L cells, respectively (left panel). Comparison of upregulated genes in three clones shows an overlap of 64 genes commonly upregulated in *TMPRSS2:ERG*-expressing PC3c cells compared to control cells. Green Venn diagram illustrates 864 genes, 179 genes and 90 genes downregulated in H, M and L cells, respectively (right panel). The 62 genes located in the overlap are common downregulated genes in *TMPRSS2:ERG*-expressing PC3c cells compared to control cells. (**b**) Common genes associated with *TMPRSS2:ERG* ectopic expression in H, M, and L cells. Left panel: 64 upregulated genes; right panel: 62 downregulated genes. The gene expression level is presented in color and average linkage hierarchical clustering was used to ordinate profiles. (**c**) Top-ranked Gene Ontology (GO) terms analyzed using the DAVID algorithm. GO term significances are presented as histograms. Red: GO terms of the 64 common upregulated genes in H, M and L cells; Green: GO terms of the 62 common downregulated genes in H, M and L cells.

Figure 4 Upregulation of *MMP9* and *PLXNA2* in *TMPRSS2:ERG*-positive human PCa samples. (**a**) *MMP9* mRNA expression in *TMPRSS2:ERG*-positive ($n=32$) and -negative ($n=20$) PCa samples was evaluated using RT-qPCR in triplicate. Two independent experiments were performed. $P=0.0055$, two-tailed Mann-Whitney test. (**b**) *PLXNA2* mRNA expression in *TMPRSS2:ERG*-positive ($n=32$) or -negative ($n=20$) PCa samples using RT-qPCR. Two independent triplicate experiments were performed. $P<0.0001$, two-tailed Mann-Whitney test. (**c**) Scatter-plot showing relative *MMP9* mRNA expression and its corresponding *ERG* mRNA expression in primary PCa samples. $n=52$, $R=0.4287$, $P=0.0015$, two-tailed non-parametric Spearman correlation test with alpha=0.05. (**d**) Scatter-plot

showing the relative *PLXNA2* mRNA expression and its corresponding *ERG* mRNA expression in primary PCa samples. *n=52, R=0.6178, P<0.0001*, two-tailed non-parametric Spearman correlation test with alpha=0.05.

Figure 5 TMPRSS2:ERG directly and positively regulates MMP9 expression in PCa cells. (**a**) A putative ETS binding site (EBS) (black oval) was identified in the *MMP9* gene promoter region (top panel), and ChIP assays were performed to examine ERG binding in H cells and in control cells. The irrelevant *GAPDH* gene promoter (without EBS) was used for negative controls (bottom panel). The positions of primers used in ChIP assay are represented by black arrows in the top panel. (**b**) *MMP9* expression was analyzed in the PC3c clone cells using RT-qPCR. (**c**) *MMP9* gene expression was analyzed using RT-qPCR in DU145 cells with ectopic *TMPRSS2:ERG* expression. (**d**) Gelatin zymography was performed to analyze secreted MMP9 levels in PC3c clone cell conditioned mediums. Loading quantity was adjusted to total conditioned medium concentration. Three independent experiments were performed and a representative experiment is shown. (**e**) Gelatin degradation assays were performed on coverslips pre-coated with FITC-gelatin for 6 h. Ten images were taken of each coverslip and degradation surfaces were analyzed by Image J, then divided by cell number after counting DAPI- and F-Actin-positive cells to calculate relative degradation surface per cell. Results are presented as fold change of the degradation surface per cell relative to control pcDNA cells set to equal 1. Mean and SEM were calculated from two independent experiments with two coverslips each. ***P<0.001, two-tailed Mann-Whitney test. (**f**) *MMP9* gene expression was analyzed in H cells treated with control or *ERG* siRNA. The expression level in cells treated with control siRNA was normalized to 1. (**g**) Gelatin zymography showing a reduction of secreted *MMP9* levels in the conditioned medium of H cells treated with *ERG* siRNA. Two independent experiments were performed and a representative experiment is shown.

Figure 6 *PLXNA2* is directly and positively regulated by TMPRSS2:ERG in PCa cells. (**a**) A putative EBS was identified in the *PLXNA2* gene promoter (black oval) (top panel). ChIP assay was performed to examine ERG binding on this EBS in *TMPRSS2:ERG*-expressing H cells or in *TMPRSS2:ERG*-negative control cells. The irrelevant *GAPDH* gene promoter (without EBS) was used for negative controls (bottom panel). The positions of primers used in ChIP assay are represented by black arrows in the top panel. (**b**) Real-time PCR detection of *PLXNA2* expression in PC3c clone cells. (**c**) *PLXNA2* expression was analyzed in DU145 with ectopic *TMPRSS2:ERG* expression. (**d**) Analysis of *PLXNA2* expression in H cells treated with either pooled control or pooled *ERG* siRNA. The expression level in H cells treated with control siRNA was normalized to 1. (**e**) Immunofluorescent analysis (IF) of ERG and PLXNA2 expression in H cells or control cells (left panel), and in H cells treated with either pooled control siRNA or pooled *ERG* siRNA (right panel). Scale bar, 20 μm.

Figure 7 PLXNA2 contributes to TMPRSS2:ERG-induced PC3c migration and invasion. (**a**) H cells were treated with pooled control or *PLXNA2*-specific siRNA, and *PLXNA2* gene expression was analyzed by RT-qPCR. The expression level in H cells treated with control siRNA was normalized to 1. (**b**) IF analysis showing ERG and PLXNA2 expression in H cells transfected with control or *PLXNA2* siRNA. Scale bar, 20 μm. (**c**) Cell migration assays were performed using the FluoroBlok™ 8 μm pore 24-well insert system (BD Biosciences) in triplicate. *TMPRSS2:ERG*-expressing H cells were treated with control, *ERG* or *PLXNA2* siRNA for 48 h, then migration was analyzed by measuring fluorescence 16 h later. Results are presented as RFU fold change compared to cells treated with control siRNA. ****P<0.001*, One-way analysis of variance (ANOVA) with Dunnett's multiple comparison test. (**d**) Cell invasion assays were performed in triplicate on H cells, pre-treated with control, *ERG* or *PLXNA2* siRNA for 48 h, using the 8 μm pore 24 well BioCoat™

Tumor Invasion System (BD Bioscience). Results are also presented as RFU fold change compared to cells treated with control siRNA measured at 16 h later. ***$P<0.001$, **$P<0.01$, one-way analysis of variance (ANOVA) with Dunnett's multiple comparison test. (**e**) Comparison of *PLXNA2* expression profile in primary PCa (n=13) and in metastatic PCa (n=20) using the dataset from Dhanasekaran *et al.* $P=0.0002$, two-tailed Mann-Whitney test. (**f**) Comparison of *PLXNA2* expression profile in primary PCa (n=7) and in metastatic PCa (n=6) using the GDS1439 dataset. $P=0.0082$, two-tailed Mann-Whitney test. (**g**) Comparison of PLXNA2 expression profile in primary PCa (n=59) and metastatic PCa (n=35) using the GSE35988 dataset. $P<0.0001$, two-tailed Mann-Whitney test.

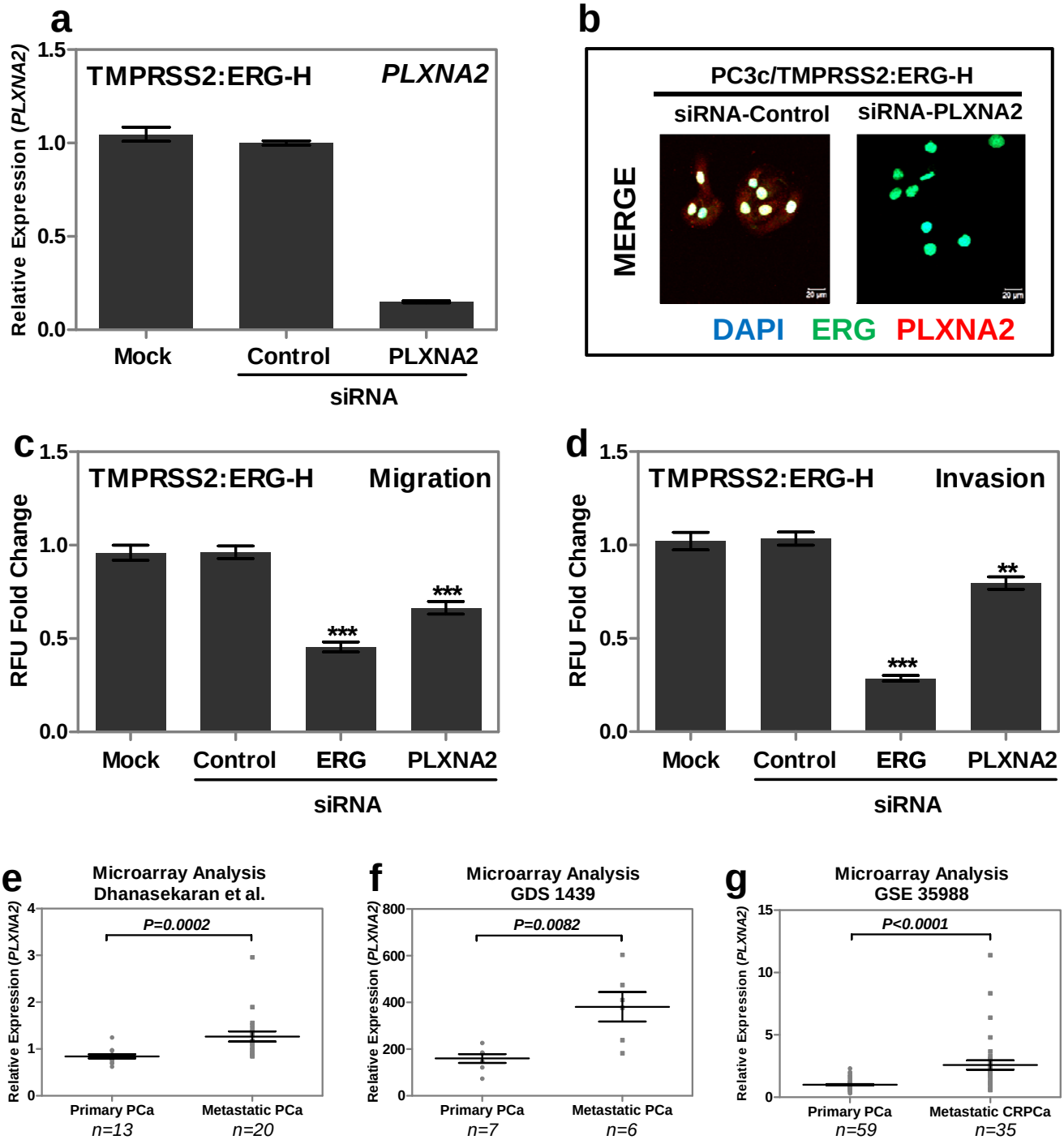
a
TMPRSS2:ERG-H
PLXNA2
Relative Expression (PLXNA2)
1.5
1.0
0.5
0.0
Mock
Control
PLXNA2
siRNA
b
PC3c/TMPRSS2:ERG-H
siRNA-Control
siRNA-PLXNA2
MERGE
DAPI
ERG
PLXNA2
c
TMPRSS2:ERG-H
Migration
RFU Fold Change
***
***
Mock
Control
ERG
PLXNA2
siRNA
d
TMPRSS2:ERG-H
Invasion
RFU Fold Change
***
**
Mock
Control
ERG
PLXNA2
siRNA
e
Microarray Analysis
Dhanasekaran et al.
Relative Expression (PLXNA2)
P=0.0002
Primary PCa
n=13
Metastatic PCa
n=20
f
Microarray Analysis
GDS 1439
Relative Expression (PLXNA2)
P=0.0082
Primary PCa
n=7
Metastatic PCa
n=6
g
Microarray Analysis
GSE 35988
Relative Expression (PLXNA2)
P<0.0001
Primary PCa
n=59
Metastatic CRPCa
n=35

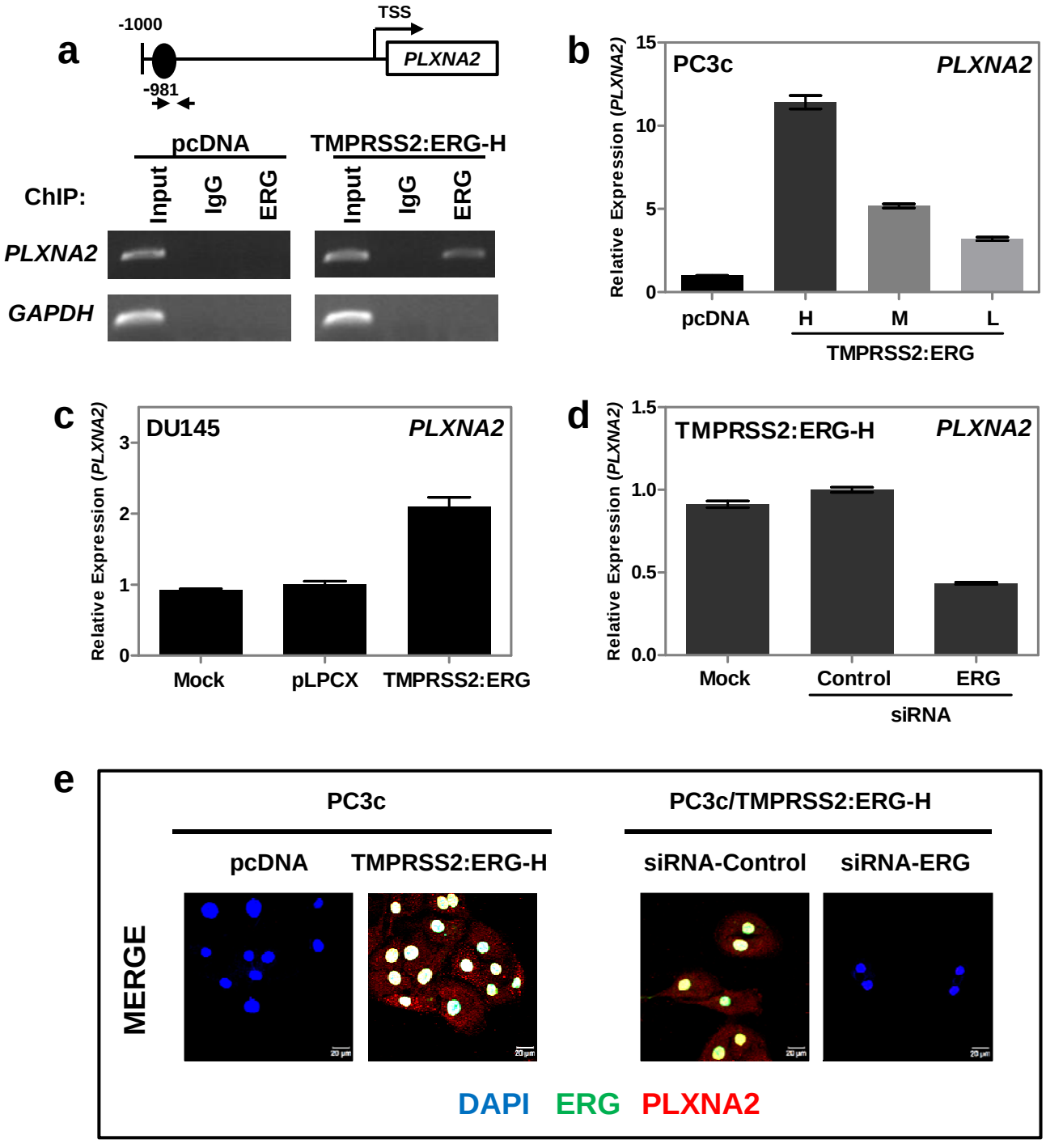
a
-1000
TSS
PLXNA2
-981
pcDNA
TMPRSS2:ERG-H
ChIP:
Input
IgG
ERG
Input
IgG
ERG
PLXNA2
GAPDH
b
PC3c
PLXNA2
Relative Expression (PLXNA2)
15
10
5
0
pcDNA
H
M
L
TMPRSS2:ERG
c
DU145
PLXNA2
Relative Expression (PLXNA2)
3
2
1
0
Mock
pLPCX
TMPRSS2:ERG
d
TMPRSS2:ERG-H
PLXNA2
Relative Expression (PLXNA2)
1.5
1.0
0.5
0.0
Mock
Control
ERG
siRNA
e
PC3c
PC3c/TMPRSS2:ERG-H
pcDNA
TMPRSS2:ERG-H
siRNA-Control
siRNA-ERG
MERGE
DAPI
ERG
PLXNA2

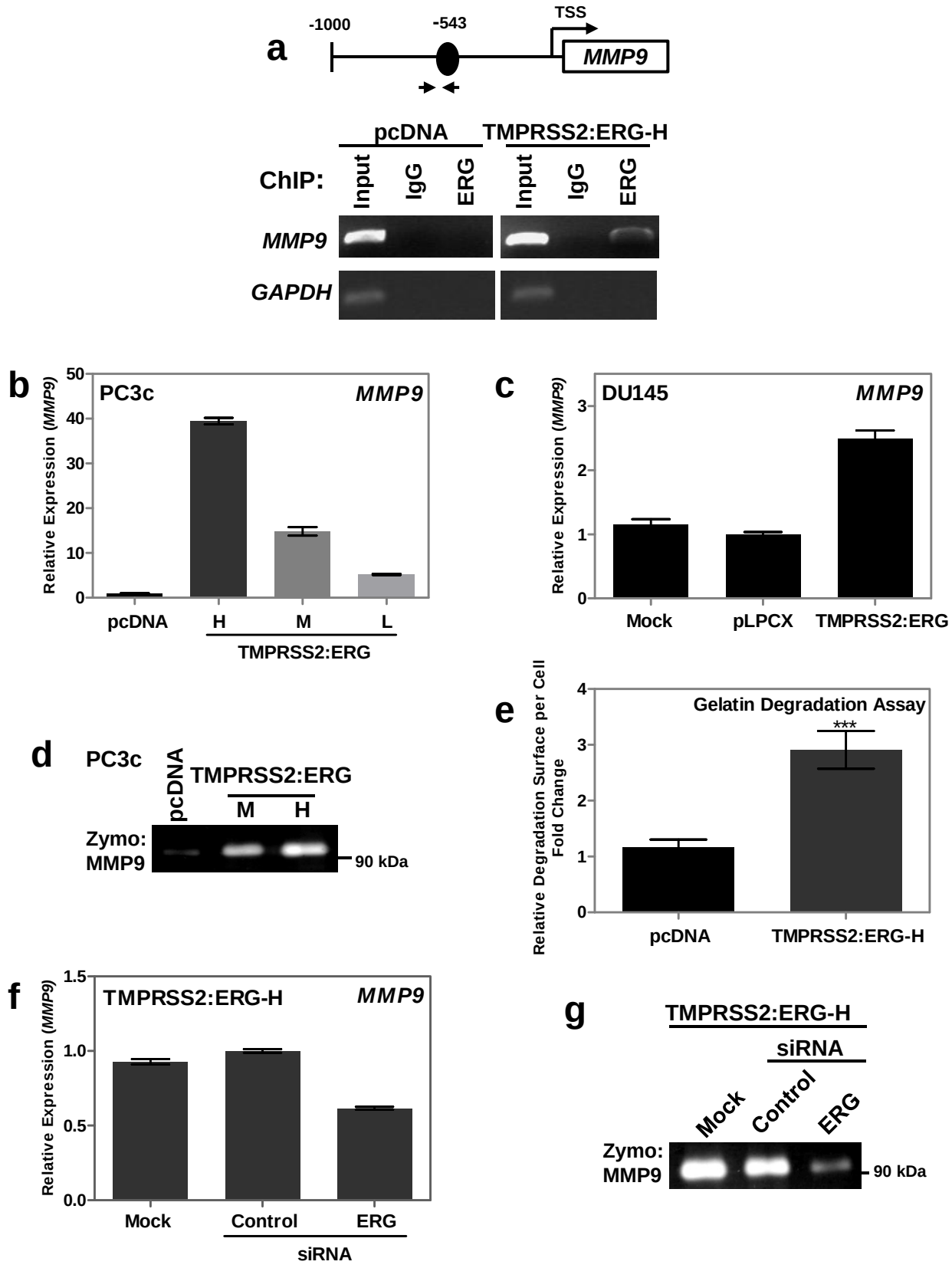
a
-1000
-543
TSS
MMP9
pcDNA
TMPRSS2:ERG-H
ChIP:
Input
IgG
ERG
Input
IgG
ERG
MMP9
GAPDH
b
PC3c
MMP9
Relative Expression (MMP9)
50
40
30
20
10
0
pcDNA
H
M
L
TMPRSS2:ERG
c
DU145
MMP9
Relative Expression (MMP9)
3
2
1
0
Mock
pLPCX
TMPRSS2:ERG
d
PC3c
pcDNA
TMPRSS2:ERG
M
H
Zymo:
MMP9
90 kDa
e
Gelatin Degradation Assay
***
Relative Degradation Surface per Cell
Fold Change
4
3
2
1
0
pcDNA
TMPRSS2:ERG-H
f
TMPRSS2:ERG-H
MMP9
Relative Expression (MMP9)
1.5
1.0
0.5
0.0
Mock
Control
ERG
siRNA
g
TMPRSS2:ERG-H
siRNA
Mock
Control
ERG
Zymo:
MMP9
90 kDa

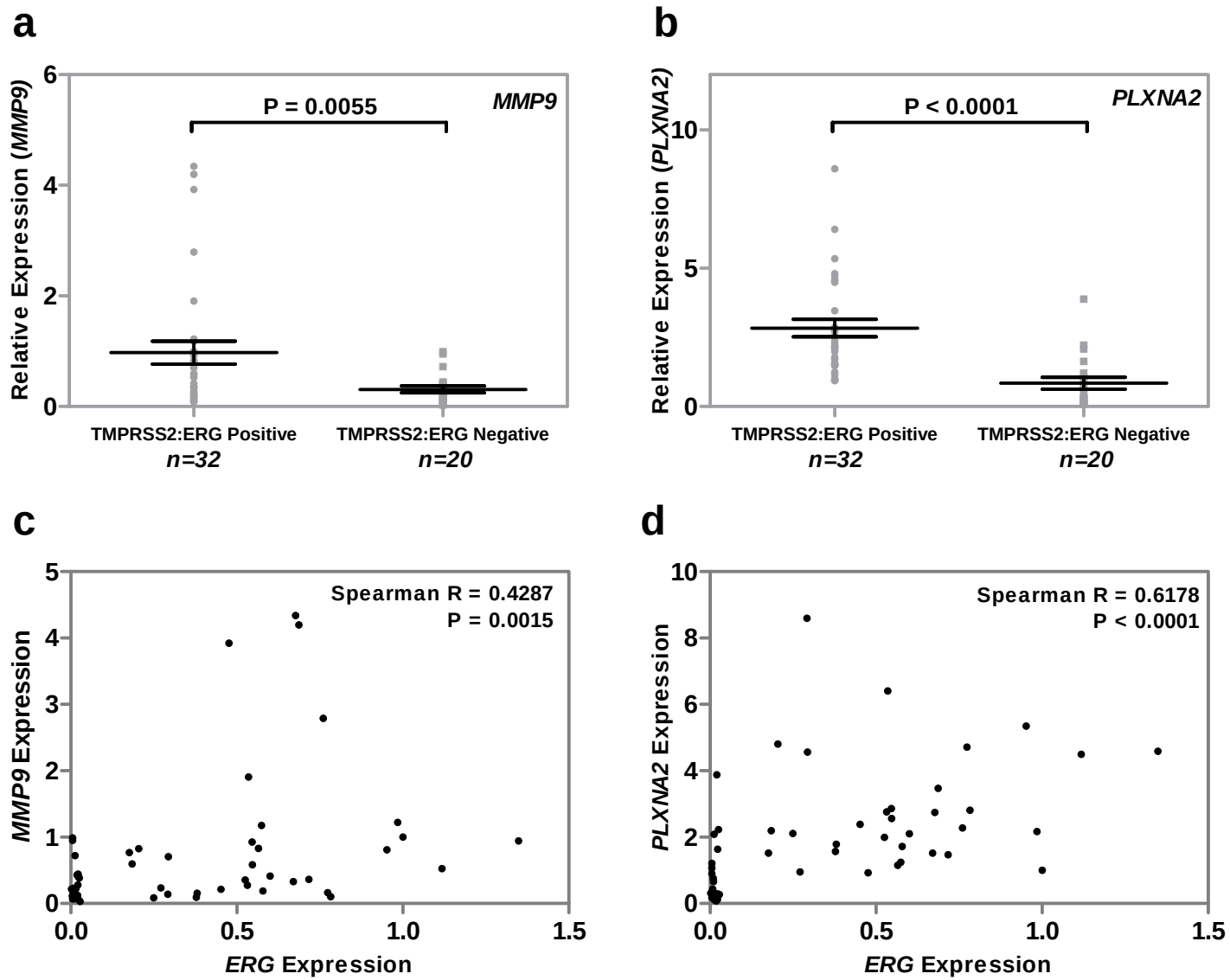
a
Relative Expression (MMP9)
P = 0.0055
MMP9
TMPRSS2:ERG Positive
n=32
TMPRSS2:ERG Negative
n=20
b
Relative Expression (PLXNA2)
P < 0.0001
PLXNA2
TMPRSS2:ERG Positive
n=32
TMPRSS2:ERG Negative
n=20
c
MMP9 Expression
Spearman R = 0.4287
P = 0.0015
ERG Expression
d
PLXNA2 Expression
Spearman R = 0.6178
P < 0.0001
ERG Expression

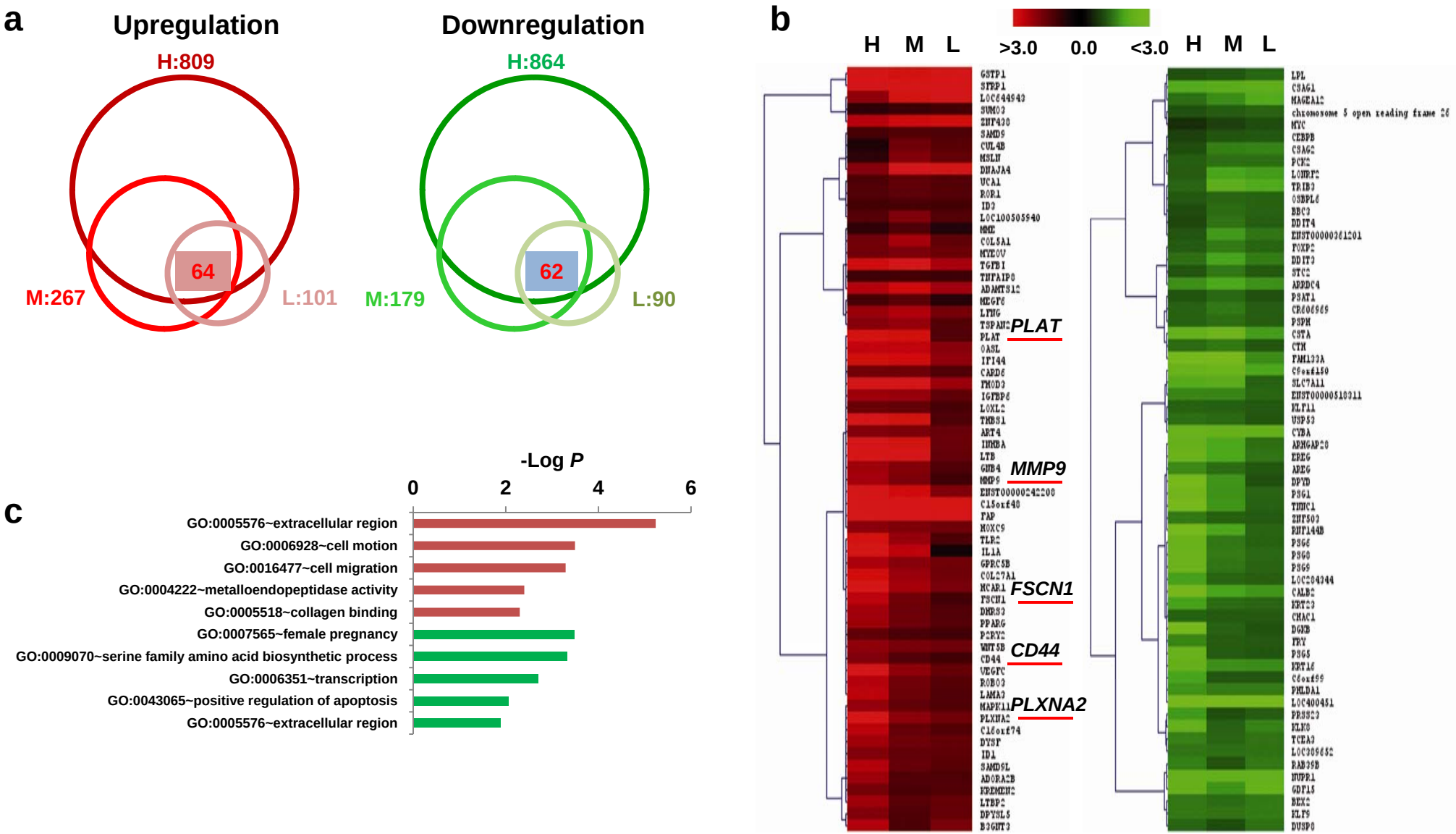
a
Upregulation
H:809
64
M:267
L:101
Downregulation
H:864
62
M:179
L:90
b
H M L
>3.0
0.0
<3.0
H M L
PLAT
MMP9
FSCN1
CD44
PLXNA2
c
-Log P
0
2
4
6
GO:0005576~extracellular region
GO:0006928~cell motion
GO:0016477~cell migration
GO:0004222~metalloendopeptidase activity
GO:0005518~collagen binding
GO:0007565~female pregnancy
GO:0009070~serine family amino acid biosynthetic process
GO:0006351~transcription
GO:0043065~positive regulation of apoptosis
GO:0005576~extracellular region

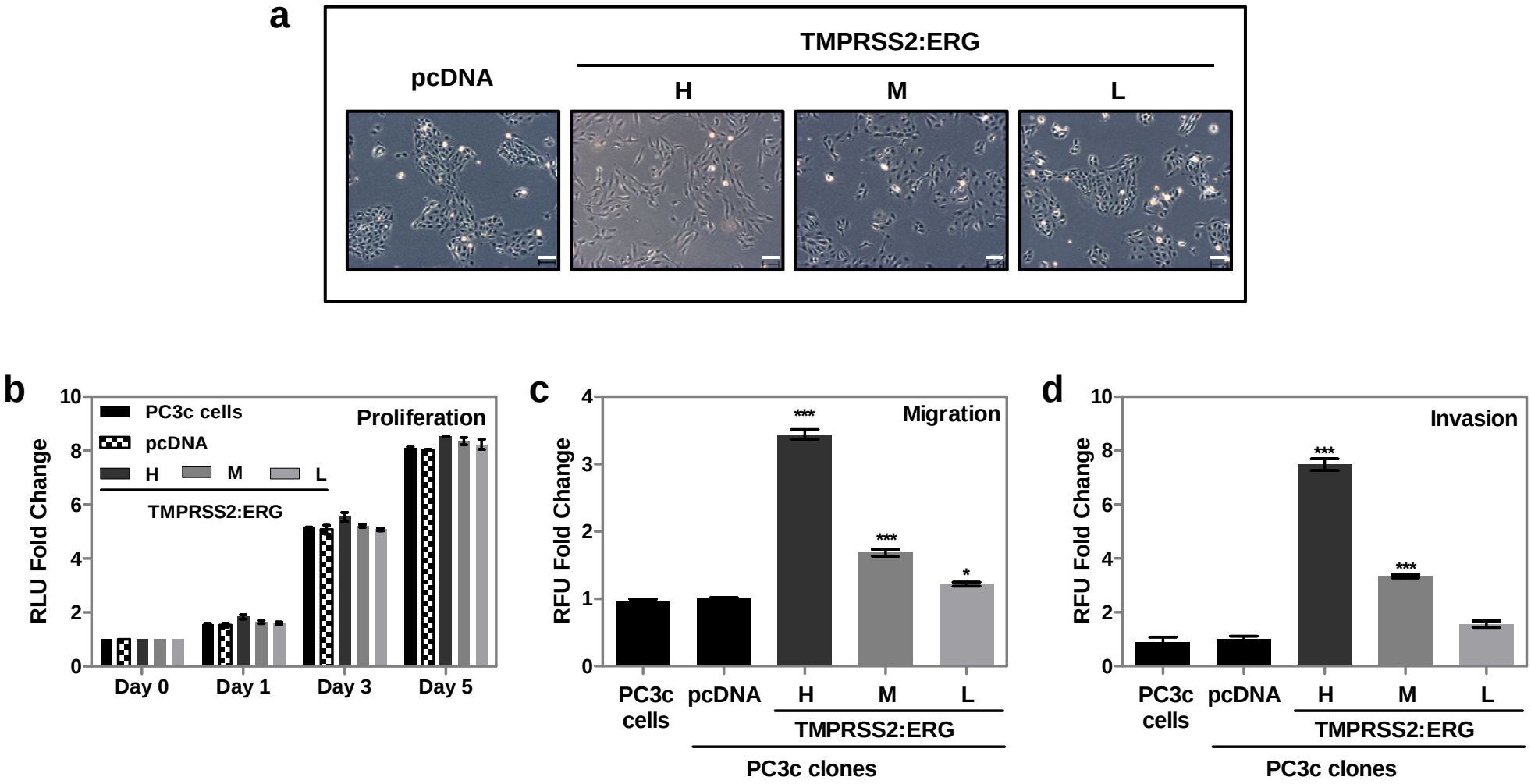
a
TMPRSS2:ERG
pcDNA
H
M
L
b
PC3c cells
pcDNA
H
M
L
TMPRSS2:ERG
Proliferation
RLU Fold Change
Day 0
Day 1
Day 3
Day 5
c
Migration
RFU Fold Change
***
***
*
PC3c cells
pcDNA
H
M
L
TMPRSS2:ERG
PC3c clones
d
Invasion
RFU Fold Change
***
***
PC3c cells
pcDNA
H
M
L
TMPRSS2:ERG
PC3c clones

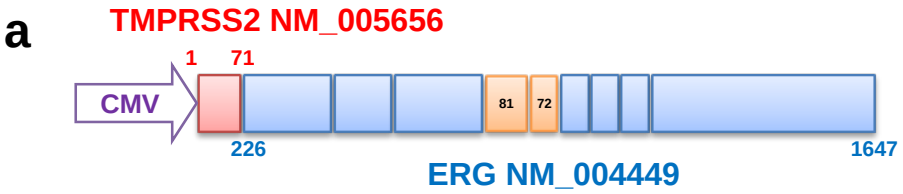
a
TMPRSS2 NM_005656
1
71
CMV
81
72
226
1647
ERG NM_004449

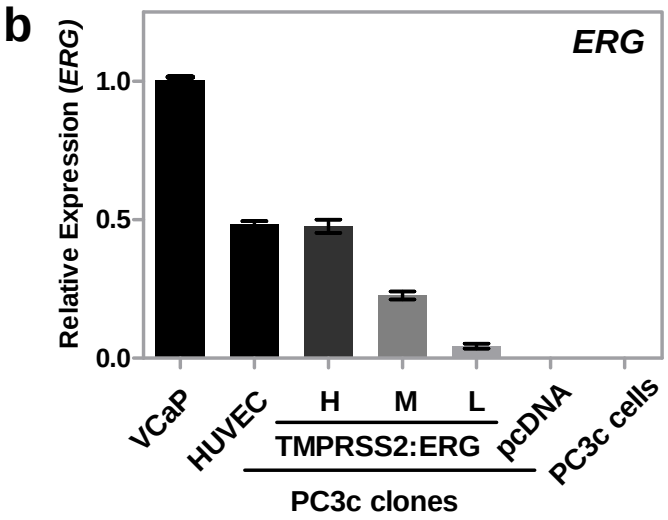
b
ERG
Relative Expression (ERG)
1.0
0.5
0.0
VCaP
HUVEC
H
M
L
pcDNA
PC3c cells
TMPRSS2:ERG
PC3c clones

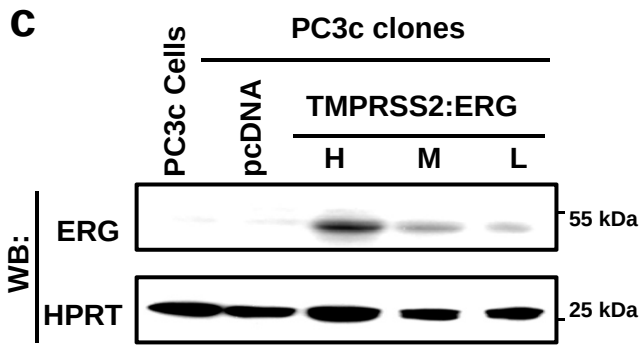
c
PC3c clones
PC3c Cells
pcDNA
TMPRSS2:ERG
H
M
L
WB:
ERG
HPRT
55 kDa
25 kDa

Supplementary Table S4: Histo-pathological Characterization of PCa Samples (n=52)

PCa Samples	TNM classification			Gleason Score	Pre-surgery PSA (ng/mL)	TMPRSS2:ERG fusion
	T	N	M			
1	T2	N0	M0	4+3	7.7	-
2	T2	N0	M0	3+3	4.51	+
3	T2	N0	M0	3+3	2.7	+
4	T2	N0	M0	3+4	4.4	+
5	T2	N0	M0	3+4	7.5	+
6	T2	N0	M0	3+4	7.21	+
7	T2	N0	M0	4+3	6.54	+
8	T2	N0	M0	3+4	9.5	+
9	T2	N0	M0	3+4	5.4	+
10	T2	N0	M0	3+3	5.38	+
11	T2	N0	M0	3+4	9.65	-
12	T2	N0	M0	3+4	7.48	+
13	T2	N0	M0	3+3	7.35	+
14	T2	N0	M0	3+3	6.26	+
15	T2	N0	M0	3+3	2.13	+
16	T2	N0	M0	3+3	5.5	-
17	T2	N0	M0	3+3	5.5	+
18	T2	N0	M0	3+3	6	+
19	T2	N0	M0	3+3	2.3	-
20	T2	N1	M0	3+3	4.79	-
21	T2	N0	M0	4+5	45.1	+
22	T3	N0	M0	4+3	6.54	+
23	T3	N0	M0	4+3	5.5	+
24	T3	N0	M0	4+5	13.1	+
25	T3	N0	M0	5+3	5.9	+
26	T3	N0	M0	3+4	224	-
27	T3	N0	M0	3+4	10	+
28	T3	N0	M0	4+3	6.9	+
29	T3	N0	M0	4+3	5	-
30	T3	N0	M0	3+4	27	-
31	T3	N0	M0	4+3	7.86	+
32	T3	N0	M0	3+4	5.9	+
33	T3	N0	M0	3+4	7.5	-
34	T3	N0	M0	3+4	5.4	+
35	T3	N0	M0	3+4	4.8	+
36	T3	N1	M1	4+5	120	-
37	T3	N1	MX	5+4	125	+
38	T3	N1	M1	5+5	563	-
39	T3	N1	M1	4+4	432	+
40	T3	N0	M0	3+3	4.72	+
41	T3	N0	M0	4+4	8.2	+
42	T3	N1	M0	4+5	169	+
43	T3	N0	M0	4+5	101	-
44	T3	N0	M0	4+5	60	-
45	T3	N1	M0	4+5	80.1	-
46	T3	N0	M0	4+5	59.2	-
47	T3	N0	M0	4+5	66.1	+
48	T3	N0	M0	4+5	101	-
49	T3	N0	M0	4+5	34	-
50	T4	N0	M0	4+5	429	-
51	T4	N1	M1	4+5	50	-
52	T4	N0	M0	5+5	79.1	-

Supplementary Table S3: 62 common downregulated genes in TMPRSS2:ERG-expressing PC3c cells

Gene Name	Probe	Gene Symbol	Annotation	H		M		L	
				Log $_2$ FC	*P value*	*Log $_2$ FC*	*P value*	*Log $_2$ FC*	*P value*
BF210146	A_32_P158376	*LOC389652*	*BF210146*	**-1,41791868**	*7,54E-05*	**-1,35322104**	*1,24E-03*	**-1,38671454**	*8,74E-03*
CR606969	A_32_P150040	*CR606969*	*CR606969*	**-1,2314649**	*2,66E-04*	**-1,44763614**	*4,24E-04*	**-1,17659944**	*6,79E-03*
NM_032523	A_32_P220762	*OSBPL6*	*Oxysterol Binding protein-like 6*	**-1,12058145**	*2,04E-03*	**-1,28085046**	*2,33E-03*	**-1,23966881**	*9,11E-03*
ENST0000036	A_24_P101651	*ENST0000036*	*ENST00000361201*	**-1,10286513**	*2,13E-03*	**-1,75148013**	*1,48E-04*	**-1,41629755**	*2,88E-03*
NM_002781	A_32_P219970	*PSG6*	*pregnancy specific beta-1-glycoprotein 5*	**-2,47159202**	*8,91E-05*	**-1,14207606**	*1,63E-03*	**-1,09511648**	*7,84E-03*
ENST0000051	A_32_P49284	*ENST0000051*	*ENST00000518311*	**-1,58372159**	*1,52E-04*	**-1,58382846**	*2,74E-04*	**-1,27794328**	*4,25E-03*
NM_000101	A_23_P163506	*CYBA*	*cytochrome b-245, alpha polypeptide*	**-2,44913037**	*7,14E-06*	**-2,4178692**	*1,31E-05*	**-2,36437005**	*3,98E-04*
NM_000110	A_23_P135548	*DPYD*	*dihydropyrimidine dehydrogenase*	**-3,03162486**	*3,29E-06*	**-1,69897541**	*3,16E-04*	**-1,05290523**	*9,43E-03*
NM_000237	A_23_P146233	*LPL*	*lipoprotein lipase*	**-1,06797162**	*2,24E-04*	**-1,12289186**	*1,81E-03*	**-1,28554578**	*3,96E-03*
NM_0010100	A_24_P579356	*ARHGAP28*	*Rho GTPase activating protein 28*	**-2,43072177**	*1,33E-05*	**-1,89550863**	*1,77E-04*	**-1,36599581**	*4,48E-03*
NM_0010424	A_24_P270728	*NUPR1*	*nuclear protein, transcriptional regulator, 1*	**-2,29528964**	*1,07E-04*	**-2,25895311**	*4,80E-05*	**-2,29344887**	*2,35E-03*
NM_0010808	A_24_P79529	*CSAG2*	*CSAG family, member 2; CSAG family, member 3; similar to CSAG family, member 2*	**-1,01216228**	*3,60E-03*	**-1,5151696**	*4,19E-04*	**-1,54606854**	*4,05E-03*
NM_0011950	A_23_P257497	*C6orf99*	*Homo sapiens chromosome 6 open reading frame 99*	**-1,85372067**	*3,74E-05*	**-1,11099989**	*2,04E-03*	**-1,09733037**	*8,08E-03*
NM_001206	A_23_P415401	*KLF9*	*Kruppel-like factor 9*	**-1,4574446**	*2,88E-05*	**-1,3958477**	*5,18E-04*	**-1,48405439**	*2,58E-03*
NM_001432	A_23_P41344	*EREG*	*epiregulin*	**-2,55901413**	*1,70E-05*	**-1,90571418**	*1,10E-04*	**-1,41329737**	*4,51E-03*
NM_001657	A_23_P259071	*AREG*	*amphiregulin; amphiregulin B*	**-1,62107875**	*2,37E-05*	**-1,33552944**	*1,18E-03*	**-1,12549374**	*8,48E-03*
NM_001740	A_23_P21092	*CALB2*	*calbindin 2*	**-2,92119518**	*4,78E-06*	**-1,85880197**	*1,16E-04*	**-1,72202989**	*1,66E-03*
NM_001902	A_23_P126103	*CTH*	*cystathionase (cystathionine gamma-lyase)*	**-1,32233196**	*3,58E-05*	**-1,4561616**	*4,15E-04*	**-1,11619076**	*7,13E-03*
NM_002467	A_23_P215956	*MYC*	*v-myc myelocytomatosis viral oncogene homolog (avian)*	**-0,63748745**	*1,47E-02*	**-0,88129184**	*7,71E-03*	**-1,02104782**	*1,18E-02*
NM_002782	A_23_P108170	*PSG6*	*pregnancy specific beta-1-glycoprotein 6*	**-2,49631972**	*5,45E-06*	**-1,44671338**	*4,25E-04*	**-1,22506964**	*6,07E-03*
NM_002784	A_23_P39309	*PSG9*	*pregnancy specific beta-1-glycoprotein 9*	**-2,57434014**	*7,45E-06*	**-1,41470487**	*1,05E-03*	**-1,25086787**	*5,20E-03*
NM_003196	A_24_P327886	*TCEA3*	*transcription elongation factor A (SII), 3*	**-1,54030146**	*1,13E-04*	**-1,26681864**	*9,45E-04*	**-1,38941773**	*4,47E-03*
NM_003280	A_23_P166823	*TNNC1*	*troponin C type 1 (slow)*	**-3,17514396**	*1,17E-06*	**-1,72710138**	*3,69E-04*	**-1,22870263**	*5,73E-03*
NM_003597	A_23_P44505	*KLF11*	*Kruppel-like factor 11*	**-1,22256751**	*7,22E-04*	**-1,20407056**	*1,22E-03*	**-1,13637723**	*7,18E-03*
NM_003714	A_23_P110686	*STC2*	*stanniocalcin 2*	**-1,10457472**	*2,16E-04*	**-1,43759507**	*4,65E-04*	**-1,14723848**	*7,13E-03*
NM_004080	A_23_P61919	*DGKB*	*diacylglycerol kinase, beta 90kDa*	**-4,03766126**	*1,87E-06*	**-1,23710948**	*1,02E-03*	**-1,07648412**	*9,22E-03*
NM_004083	A_23_P21134	*DDIT3*	*DNA-damage-inducible transcript 3*	**-1,3660376**	*7,93E-04*	**-1,85167646**	*2,16E-04*	**-1,48448283**	*2,99E-03*
NM_004420	A_23_P390528	*DUSP8*	*dual specificity phosphatase 8*	**-1,25972708**	*3,35E-03*	**-1,01322655**	*3,26E-03*	**-1,38583012**	*4,30E-03*
NM_004563	A_23_P140207	*PCK2*	*phosphoenolpyruvate carboxykinase 2 (mitochondrial)*	**-1,18098063**	*6,73E-04*	**-1,37479311**	*5,52E-04*	**-1,35664248**	*3,35E-03*
NM_004577	A_23_P251984	*PSPH*	*phosphoserine phosphatase-like; phosphoserine phosphatase*	**-1,2359542**	*2,30E-04*	**-1,35077206**	*6,05E-04*	**-1,1716885**	*5,79E-03*
NM_004864	A_23_P16523	*GDF15*	*growth differentiation factor 15*	**-2,42366784**	*8,20E-05*	**-1,69858499**	*4,38E-04*	**-2,39238588**	*4,29E-04*
NM_005194	A_23_P411296	*CEBPB*	*CCAAT/enhancer binding protein (C/EBP), beta*	**-0,87343114**	*2,89E-03*	**-1,10199141**	*2,75E-03*	**-1,12832902**	*7,56E-03*
NM_005213	A_23_P170233	*CSTA*	*cystatin A (stefin A)*	**-2,28500829**	*3,30E-05*	**-2,66372862**	*8,38E-06*	**-1,78687604**	*1,39E-03*
NM_005367	A_23_P252928	*MAGEA12*	*melanoma antigen family A, 12*	**-1,35694933**	*1,31E-03*	**-1,64465938**	*3,13E-04*	**-2,00564759**	*5,07E-04*
NM_005557	A_23_P38537	*KRT16*	*keratin 16; keratin type 16-like*	**-2,35504973**	*1,18E-05*	**-1,65904918**	*3,56E-04*	**-1,63495607**	*2,17E-03*
NM_006905	A_23_P50697	*PSG1*	*pregnancy specific beta-1-glycoprotein 1*	**-2,84056045**	*3,20E-06*	**-1,69333899**	*1,85E-04*	**-1,2473813**	*4,48E-03*
NM_007173	A_24_P937405	*PRSS23*	*protease, serine, 23*	**-1,76082169**	*1,96E-05*	**-1,03313193**	*2,87E-03*	**-1,17759475**	*5,71E-03*
NM_007350	A_23_P76450	*PHLDA1*	*pleckstrin homology-like domain, family A, member 1*	**-1,69903751**	*3,40E-05*	**-1,4769497**	*3,89E-04*	**-1,4811118**	*2,35E-03*
NM_014331	A_32_P165477	*SLC7A11*	*solute carrier family 7, (cationic amino acid transporter, y+ system) member 11*	**-2,08047468**	*6,45E-06*	**-2,14489415**	*3,86E-05*	**-1,23562508**	*4,67E-03*
NM_014417	A_23_P382775	*BBC3*	*BCL2 binding component 3*	**-1,00732159**	*4,17E-04*	**-1,33654378**	*6,77E-04*	**-1,23073552**	*4,85E-03*
NM_015515	A_23_P78248	*KRT23*	*keratin 23 (histone deacetylase inducible)*	**-1,83350968**	*1,85E-05*	**-1,32441993**	*6,83E-04*	**-1,26026537**	*4,35E-03*
NM_019050	A_24_P137522	*USP53*	*ubiquitin specific peptidase 53*	**-1,35699793**	*1,87E-04*	**-1,29991961**	*8,52E-04*	**-1,09717863**	*9,11E-03*
NM_019058	A_23_P104318	*DDIT4*	*DNA-damage-inducible transcript 4*	**-0,92606048**	*3,03E-04*	**-1,3922176**	*5,19E-04*	**-1,19533261**	*5,31E-03*
NM_021158	A_24_P305541	*TRIB3*	*tribbles homolog 3 (Drosophila)*	**-1,26830874**	*3,14E-03*	**-2,22619136**	*1,48E-04*	**-1,99878018**	*1,79E-03*

Supplementary Table S3: 62 common downregulated genes in TMPRSS2:ERG-expressing PC3c cells

Gene Name	Probe	Gene Symbol	Annotation	H		M		L	
				Log $_2$ FC	*P value*	*Log $_2$ FC*	*P value*	*Log $_2$ FC*	*P value*
NM_023037	A_23_P105862	*FRY*	*furry homolog (Drosophila)*	**-1,58604354**	*1,74E-04*	**-1,15620552**	*1,97E-03*	**-1,14045508**	*7,02E-03*
NM_024111	A_23_P14863	*CHAC1*	*ChaC, cation transport regulator homolog 1 (E. coli)*	**-1,23800755**	*9,10E-05*	**-1,14978915**	*1,88E-03*	**-1,14312725**	*6,96E-03*
NM_032621	A_23_P22735	*BEX2*	*brain expressed X-linked 2*	**-1,43746385**	*1,97E-05*	**-1,33027821**	*6,84E-04*	**-1,46674838**	*2,53E-03*
NM_032772	A_23_P202484	*ZNF503*	*zinc finger protein 503*	**-1,46634134**	*3,01E-04*	**-1,2218935**	*1,21E-03*	**-1,14919162**	*6,32E-03*
NM_058179	A_23_P259692	*PSAT1*	*chromosome 8 open reading frame 62; phosphoserine aminotransferase 1*	**-1,09216315**	*3,70E-04*	**-1,2851445**	*1,33E-03*	**-1,06783684**	*9,49E-03*
NM_144505	A_23_P369343	*KLK8*	*kallikrein-related peptidase 8*	**-2,3099324**	*7,71E-04*	**-1,23426937**	*1,08E-03*	**-1,54530491**	*2,88E-03*
NM_148898	A_24_P38316	*FOXP2*	*forkhead box P2*	**-1,16257205**	*3,45E-04*	**-1,46460559**	*4,79E-04*	**-1,27051843**	*5,70E-03*
NM_153478	A_24_P11061	*CSAG1*	*chondrosarcoma associated gene 1*	**-2,00142153**	*1,89E-04*	**-2,09838797**	*3,03E-04*	**-2,23168982**	*2,25E-04*
NM_171998	A_24_P408603	*RAB39B*	*RAB39B, member RAS oncogene family*	**-1,52450725**	*2,86E-04*	**-1,09278857**	*2,07E-03*	**-1,45376668**	*2,98E-03*
NM_173698	A_23_P345808	*FAM133A*	*family with sequence similarity 133, member A*	**-4,08705351**	*1,87E-06*	**-5,63321118**	*8,88E-06*	**-1,64580833**	*1,77E-03*
NM_182707	A_24_P392110	*PSG8*	*pregnancy specific beta-1-glycoprotein 7; pregnancy specific beta-1-glycoprotein 8; pregnancy specific b*	**-2,52811923**	*4,24E-06*	**-1,47525321**	*4,15E-04*	**-1,2884775**	*3,96E-03*
NM_182757	A_24_P406060	*RNF144B*	*ring finger protein 144B*	**-3,98861218**	*1,23E-06*	**-1,88007321**	*1,21E-04*	**-1,25415931**	*7,31E-03*
NM_183376	A_23_P339818	*ARRDC4*	*arrestin domain containing 4*	**-1,6682404**	*1,67E-03*	**-1,93675889**	*7,42E-05*	**-1,68108966**	*2,36E-03*
NM_198461	A_32_P190303	*LONRF2*	*LON peptidase N-terminal domain and ring finger 2*	**-1,16022619**	*1,47E-03*	**-1,86532483**	*1,88E-04*	**-1,77632568**	*1,17E-03*
NM_203403	A_23_P83007	*C9orf150*	*chromosome 9 open reading frame 150*	**-2,51188422**	*3,88E-04*	**-2,60612569**	*9,67E-06*	**-1,9019306**	*1,29E-03*
NM_207446	A_23_P100001	*LOC400451*	*family with sequence similarity 174, member B*	**-4,1202078**	*7,05E-06*	**-3,04001545**	*5,89E-06*	**-3,07287002**	*5,25E-05*
NR_015370	A_23_P58538	*chromosome*	*chromosome 5 open reading frame 26*	**-1,05905921**	*1,95E-04*	**-1,17500604**	*1,40E-03*	**-1,24873723**	*4,90E-03*
NR_033888	A_24_P882959	*LOC284344*	*Homo sapiens uncharacterized LOC284344 (LOC284344), non-coding RNA*	**-1,81421343**	*7,95E-05*	**-1,26512158**	*1,25E-03*	**-1,18898504**	*9,21E-03*

Supplementary Table S2: 64 common upregulated genes in TMPRSS2:ERG-expressing PC3c cells

Gene Name	Probe	Gene Symbol	Annotation	H		M		L	
				Log $_2$ FC	*P value*	*Log $_2$ FC*	*P value*	*Log $_2$ FC*	*P value*
ENST0000024	A_24_P535256	*ENST0000024*	*ENST00000242208*	**3,4495517**	*9,72E-06*	**2,75864448**	*1,05E-05*	**1,82524492**	*0,00217015*
NM_005012	A_32_P4018	*ROR1*	*receptor tyrosine kinase-like orphan receptor 1*	**1,30283884**	*0,0010761*	**1,4226011**	*0,00084521*	**1,32838946**	*0,0034485*
NM_032554	A_23_P394246	*HCAR1*	*hydroxycarboxylic acid receptor 1*	**3,13840381**	*1,40E-05*	**2,27924136**	*7,35E-05*	**1,74639699**	*0,00119794*
NM_032888	A_23_P158096	*COL27A1*	*collagen, type XXVII, alpha 1*	**2,81024944**	*3,29E-06*	**2,12891847**	*5,87E-05*	**1,63171763**	*0,00252617*
NM_000093	A_23_P158593	*COL5A1*	*collagen, type V, alpha 1*	**1,64029408**	*0,00014023*	**2,26156607**	*2,37E-05*	**1,44663007**	*0,00334751*
NM_000358	A_23_P156327	*TGFBI*	*transforming growth factor, beta-induced, 68kDa*	**2,80880325**	*3,68E-05*	**3,81845776**	*3,82E-06*	**2,3140582**	*0,00021414*
NM_000428	A_23_P218144	*LTBP2*	*latent transforming growth factor beta binding protein 2*	**2,193703**	*0,00032987*	**1,36893566**	*0,0006058*	**1,50946873**	*0,00447424*
NM_000575	A_23_P72096	*IL1A*	*interleukin 1, alpha*	**4,86449141**	*1,87E-06*	**2,52702853**	*1,05E-05*	**0,49369335**	*0,2022043*
NM_000610	A_23_P24870	*CD44*	*CD44 molecule (Indian blood group)*	**1,82579518**	*4,54E-05*	**1,29534947**	*0,00079437*	**1,06257404**	*0,00973226*
NM_000676	A_23_P55477	*ADORA2B*	*hypothetical LOC100131909; adenosine A2b receptor*	**2,15785283**	*7,05E-06*	**1,27540873**	*0,00117234*	**1,21517596**	*0,00497849*
NM_000852	A_23_P202658	*GSTP1*	*glutathione S-transferase pi 1*	**3,20785566**	*3,34E-05*	**2,89560413**	*1,15E-05*	**5,56786645**	*6,37E-06*
NM_000930	A_23_P82868	*PLAT*	*plasminogen activator, tissue*	**2,92014795**	*2,23E-06*	**2,86176488**	*5,44E-06*	**1,26695125**	*0,00445263*
NM_0010401	A_23_P8452	*LFNG*	*LFNG O-fucosylpeptide 3-beta-N-acetylglucosaminyltransferase*	**2,14012398**	*1,47E-05*	**2,36719695**	*1,70E-05*	**1,70620911**	*0,00132041*
NM_0010805	A_32_P52414	*LOC644943*	*Ras association (RalGDS/AF-6) domain family (N-terminal) member 10*	**2,01940409**	*0,00123561*	**2,90719901**	*1,06E-05*	**3,4273124**	*5,12E-05*
NM_001409	A_24_P926960	*MEGF6*	*multiple EGF-like-domains 6*	**1,1308263**	*0,00118809*	**1,38102082**	*0,00074941*	**0,74476166**	*0,04080211*
NM_002165	A_23_P252306	*ID1*	*inhibitor of DNA binding 1, dominant negative helix-loop-helix protein*	**1,85010354**	*1,62E-05*	**1,4674131**	*0,00047408*	**1,40446158**	*0,00295129*
NM_002167	A_23_P137381	*ID3*	*inhibitor of DNA binding 3, dominant negative helix-loop-helix protein*	**1,13698227**	*0,00014229*	**1,17194042**	*0,00168606*	**1,13781983**	*0,00659747*
NM_002178	A_23_P139912	*IGFBP6*	*insulin-like growth factor binding protein 6*	**2,17737016**	*4,40E-06*	**2,08349049**	*5,67E-05*	**1,42906818**	*0,00312489*
NM_002192	A_23_P122924	*INHBA*	*inhibin, beta A*	**3,34695573**	*4,45E-06*	**2,91142459**	*5,44E-06*	**1,55485994**	*0,0020654*
NM_002318	A_23_P111995	*LOXL2*	*lysyl oxidase-like 2*	**1,57115991**	*3,56E-05*	**1,48596967**	*0,00039221*	**1,16303028**	*0,00597385*
NM_002341	A_23_P93348	*LTB*	*lymphotoxin beta (TNF superfamily, member 3)*	**4,38910213**	*2,83E-06*	**3,43222314**	*5,44E-06*	**1,50379139**	*0,00306967*
NM_002751	A_23_P502274	*MAPK11*	*mitogen-activated protein kinase 11*	**2,06921509**	*1,64E-05*	**1,46188256**	*0,00041398*	**1,26296329**	*0,00593456*
NM_003012	A_23_P10127	*SFRP1*	*secreted frizzled-related protein 1*	**3,38233813**	*7,65E-06*	**3,29062341**	*5,44E-06*	**5,14603198**	*6,37E-06*
NM_003088	A_23_P168531	*FSCN1*	*fascin homolog 1, actin-bundling protein (Strongylocentrotus purpuratus)*	**2,50677701**	*3,46E-05*	**1,62291075**	*0,00035597*	**1,09130434**	*0,00876387*
NM_003246	A_23_P206212	*THBS1*	*thrombospondin 1*	**3,37607996**	*1,95E-05*	**2,91622092**	*5,44E-06*	**1,22455685**	*0,0063206*
NM_003264	A_23_P92499	*TLR2*	*toll-like receptor 2*	**2,904175**	*3,24E-05*	**2,08635311**	*0,00013044*	**1,21870916**	*0,00489826*
NM_003494	A_23_P39925	*DYSF*	*dysferlin, limb girdle muscular dystrophy 2B (autosomal recessive)*	**2,1937892**	*1,40E-05*	**1,63096776**	*0,00025711*	**1,49991476**	*0,00236278*
NM_003588	A_23_P422178	*CUL4B*	*cullin 4B*	**0,64342805**	*0,00745917*	**1,62356929**	*0,00028589*	**1,3598221**	*0,00312222*
NM_003733	A_23_P139786	*OASL*	*2'-5'-oligoadenylate synthetase-like*	**2,57422695**	*8,44E-05*	**2,54860934**	*9,02E-06*	**1,91915364**	*0,00095544*
NM_004460	A_23_P56746	*FAP*	*fibroblast activation protein, alpha*	**5,39496843**	*9,05E-07*	**4,77699852**	*2,16E-06*	**4,02339409**	*1,85E-05*
NM_004753	A_23_P33759	*DHRS3*	*dehydrogenase/reductase (SDR family) member 3*	**2,20445645**	*3,34E-05*	**1,60821553**	*0,00027451*	**1,27020485**	*0,00428201*
NM_004994	A_23_P40174	*MMP9*	*matrix metallopeptidase 9 (gelatinase B, 92kDa gelatinase, 92kDa type IV collagenase)*	**2,24730803**	*2,83E-06*	**1,77389168**	*0,00015004*	**1,04873192**	*0,00940379*
NM_005429	A_23_P167096	*VEGFC*	*vascular endothelial growth factor C*	**3,1671143**	*2,71E-06*	**2,00963852**	*0,00024478*	**1,52382508**	*0,00285125*
NM_005725	A_23_P201193	*TSPAN2*	*tetraspanin 2*	**1,90595797**	*5,32E-05*	**2,10056978**	*5,06E-05*	**1,31110511**	*0,00370411*
NM_005823	A_23_P77529	*MSLN*	*mesothelin*	**0,80726104**	*0,00547454*	**1,8557777**	*0,00013593*	**1,48933316**	*0,00283113*
NM_006417	A_23_P23074	*IFI44*	*interferon-induced protein 44*	**2,87859612**	*1,06E-05*	**2,79779509**	*5,89E-06*	**2,03208076**	*0,00044277*
NM_006897	A_23_P25150	*HOXC9*	*homeobox C9*	**1,94806845**	*0,00023853*	**1,80660472**	*0,0002962*	**1,63448271**	*0,0036561*
NM_006936	A_23_P102937	*SUMO3*	*SMT3 suppressor of mif two 3 homolog 2 (S. cerevisiae) pseudogene; SMT3 suppressor of mif two*	**0,8361159**	*0,00410646*	**1,01719451**	*0,00367611*	**1,117685**	*0,00712696*
NM_007289	A_24_P260101	*MME*	*membrane metallo-endopeptidase*	**0,8168381**	*0,00693129*	**1,24306003**	*0,00105343*	**0,7019343**	*0,05419134*
NM_014256	A_23_P78980	*B3GNT3*	*UDP-GlcNAc:betaGal beta-1,3-N-acetylglucosaminyltransferase 3*	**2,39803785**	*7,14E-06*	**1,21272689**	*0,00125079*	**1,77586456**	*0,00121201*
NM_014350	A_32_P219520	*TNFAIP8*	*tumor necrosis factor, alpha-induced protein 8*	**1,06953295**	*0,00114313*	**1,09599389**	*0,00331229*	**1,05042516**	*0,00941858*
NM_016235	A_23_P324327	*GPRC5B*	*G protein-coupled receptor, family C, group 5, member B*	**2,32040176**	*3,83E-05*	**1,92159657**	*7,94E-05*	**1,6169327**	*0,00543052*
NM_017654	A_23_P355244	*SAMD9*	*sterile alpha motif domain containing 9*	**1,15433736**	*0,00031326*	**1,27265962**	*0,00087128*	**1,2459451**	*0,00629024*
NM_018602	A_23_P206140	*DNAJA4*	*DnaJ (Hsp40) homolog, subfamily A, member 4*	**1,90273976**	*0,00250654*	**4,03422988**	*3,13E-06*	**2,96510379**	*0,00015874*

Supplementary Table S2: 64 common upregulated genes in TMPRSS2:ERG-expressing PC3c cells

Gene Name	Probe	Gene Symbol	Annotation	H		M		L	
				Log $_2$ FC	*P value*	*Log $_2$ FC*	*P value*	*Log $_2$ FC*	*P value*
NM_020134	A_23_P210224	*DPYSL5*	*dihydropyrimidinase-like 5*	**1,84146402**	*1,64E-05*	**1,22727201**	*0,00111669*	**1,47884867**	*0,00234838*
NM_021071	A_23_P116902	*ART4*	*ADP-ribosyltransferase 4 (Dombrock blood group)*	**1,849363**	*0,00787111*	**1,77604652**	*0,00031777*	**1,53876511**	*0,00306597*
NM_021629	A_32_P171313	*GNB4*	*guanine nucleotide binding protein (G protein), beta polypeptide 4*	**2,18971734**	*1,85E-05*	**1,87336873**	*0,00010921*	**1,2461904**	*0,00447424*
NM_022370	A_23_P356581	*ROBO3*	*roundabout, axon guidance receptor, homolog 3 (Drosophila)*	**2,4008704**	*4,54E-05*	**1,64022292**	*0,00047275*	**1,33342014**	*0,00343007*
NM_025135	A_32_P34444	*FHOD3*	*formin homology 2 domain containing 3*	**4,10351737**	*1,07E-05*	**3,86856762**	*5,44E-06*	**2,15478103**	*0,00166461*
NM_025179	A_23_P46618	*PLXNA2*	*plexin A2*	**3,19528483**	*5,96E-06*	**1,96905162**	*6,77E-05*	**1,61377018**	*0,00287726*
NM_030775	A_23_P53588	*WNT5B*	*wingless-type MMTV integration site family, member 5B*	**2,03949498**	*0,00055932*	**1,74557366**	*0,00038816*	**1,61532611**	*0,0016596*
NM_030955	A_32_P103220	*ADAMTS12*	*ADAM metallopeptidase with thrombospondin type 1 motif, 12*	**2,44605665**	*2,05E-05*	**2,74427443**	*5,93E-06*	**2,21406233**	*0,00022686*
NM_032413	A_23_P26024	*C15orf48*	*chromosome 15 open reading frame 48*	**5,8889039**	*9,05E-07*	**4,59532803**	*2,16E-06*	**2,95210513**	*5,25E-05*
NM_032587	A_23_P41854	*CARD6*	*caspase recruitment domain family, member 6*	**1,63727421**	*7,72E-05*	**1,59568454**	*0,00038816*	**1,26003906**	*0,0063206*
NM_138711	A_23_P252062	*PPARG*	*peroxisome proliferator-activated receptor gamma*	**2,178288**	*1,14E-05*	**1,60375259**	*0,00038238*	**1,32264733**	*0,00376812*
NM_138768	A_23_P360240	*MYEOV*	*myeloma overexpressed (in a subset of t(11;14) positive multiple myelomas)*	**1,6338799**	*0,00027*	**1,78456231**	*0,00013592*	**1,5658368**	*0,00267157*
NM_152703	A_23_P145874	*SAMD9L*	*sterile alpha motif domain containing 9-like*	**2,40778834**	*8,87E-06*	**1,5074545**	*0,00037234*	**1,34942225**	*0,00699606*
NM_172229	A_23_P77612	*KREMEN2*	*kringle containing transmembrane protein 2*	**1,68625263**	*1,81E-05*	**1,21097049**	*0,00114599*	**1,27440774**	*0,00543052*
NM_176072	A_23_P24903	*P2RY2*	*purinergic receptor P2Y, G-protein coupled, 2*	**1,47009792**	*4,60E-05*	**1,1897628**	*0,00125637*	**1,06418491**	*0,00917063*
NM_182755	A_23_P161156	*ZNF438*	*zinc finger protein 438*	**2,47978681**	*5,85E-05*	**2,72025567**	*0,00013848*	**2,83450713**	*6,26E-05*
NM_198129	A_24_P687302	*LAMA3*	*laminin, alpha 3*	**2,51712884**	*2,07E-05*	**1,58203896**	*0,00099137*	**1,22698646**	*0,01184986*
NM_206967	A_24_P289178	*C16orf74*	*chromosome 16 open reading frame 74*	**2,50235533**	*2,32E-06*	**1,51491943**	*0,000344*	**1,27585318**	*0,00478496*
NR_015379	A_32_P200238	*UCA1*	*urothelial cancer associated 1*	**1,2258268**	*8,12E-05*	**1,45323115**	*0,00041949*	**1,28564612**	*0,00412749*
XR_110477	A_32_P158019	*LOC10050594*	*PREDICTED: Homo sapiens uncharacterized LOC100505940*	**1,3192231**	*0,00046213*	**1,83220714**	*0,0002962*	**1,29626969**	*0,00643079*

Supplementary Table S1: Oligonucleotide Primers

Primer	Direction	Sequence	Reference
TMPRSS2 :ERG **(Cloning)**	**Forward**	**5'- CGCGAGCTAAGCAGGAGGC -3'**	**This study**
	Reverse	**5'- CCTCCGCCAGGTCTTTAGTA -3'**	
TMPRSS2:ERG **(Classical PCR)**	**Forward**	**5'- CGCGAGCTAAGCAGGAGGC -3'**	**(1)**
	Reverse	**5'- GTAGGCACACTCAAACAACGACTGG- 3'**	
ERG **(qPCR)**	**Forward**	**5'- AACGAGCGCAGAGTTATCGT -3'**	**This study**
	Reverse	**5'- GTGAGCCTCTGGAAGTCGTC -3'**	**(Effeciency: 99.8%)**
MMP9 **(qPCR)**	**Forward**	**5'- AAGTGGCACCACCACAACATC -3'**	**(2)**
	Reverse	**5'- CAAAGGCGTCGTCAATCACC -3'**	**(Effeciency: 98.3%)**
PLXNA2 **(qPCR)**	**Forward**	**5'-GGAGCCACTCTTCATGCTATACTGT-3'**	**(3)**
	Reverse	**5'- GTTGACGCAGTTCAGGATCA-3'**	**(Effeciency: 99.1%)**
18s **(qPCR)**	**Forward**	**5'- CAGCTTCCGGGAAACCAAAGTC-3'**	**(4)**
	Reverse	**5'- AATTAAGCCGCAGGCTCCACTC-3'**	
pMMP9 **(ChIP)**	**Forward**	**5'- TGCGGACTTACAACCTACAGTG-3'**	**(5)**
	Reverse	**5'- TCTTTGACTCAGCTTCCTCTCC-3'**	
pPLXNA2 **(ChIP)**	**Forward**	**5'- CCGCTTCCGGAAAGCCGTGT-3'**	**This study**
	Reverse	**5'- GTCCCGACTTGCATGGGGGC-3'**	
pGAPDH (ChIP)	**Forward**	**5'- GCGTGCCCAGTTGAACCA-3'**	**(6)**
	Reverse	**5'- CGCCCGTAAAACCGCTAGT-3'**	
CHD1 **(qPCR)**	**Forward**	**5'- CCCACCACGTACAAGGGTC-3'**	*** (Effeciency: 99.3%)**
	Reverse	**5'- CTGGGGTATTGGGGGCAT-3'**	
VIM **(qPCR)**	**Forward**	**5'- GAGAACTTTGCCGTTGAAGC-3'**	*** (Effeciency: 97.6%)**
	Reverse	**5'- GCTTCCTGTAGGTGGCAATC-3'**	
TWIST1 **(qPCR)**	**Forward**	**5'-GCAGGACGTGTCCAGCTC-3'**	*** (Effeciency: 99.1%)**
	Reverse	**5'- CTGGCTCTTCCTCGCTGTT-3'**	

Primer	Direction	Sequence	Reference
***SNAI1/SNAIL* (qPCR)**	**Forward**	**5'- AATCGGAAGCCTAACTACAGCG-3'**	*** (Effeciency: 96.3%)**
	Reverse	**5'- GTCCCAGATGAGCATTGGCAA-3'**	
***SNAI2/SLUG* (qPCR)**	**Forward**	**5'- ATACCACAACCAGAGATCCTCA-3'**	*** (Effeciency: 99.8%)**
	Reverse	**5'- GACTCACTCGCCCCAAAGATG-3'**	

* These primers have been cited by multiple publications.

1. Tomlins SA, Rhodes DR, Perner S, Dhanasekaran SM, Mehra R, Sun XW, et al. Recurrent fusion of TMPRSS2 and ETS transcription factor genes in prostate cancer. Science. 2005 Oct 28;310(5748):644-8.
2. Kato T, Fujita Y, Nakane K, Kojima T, Nozawa Y, Deguchi T, et al. ETS1 promotes chemoresistance and invasion of paclitaxel-resistant, hormone-refractory PC3 prostate cancer cells by up-regulating MDR1 and MMP9 expression. Biochem Biophys Res Commun. 2012 Jan 20;417(3):966-71.
3. Gabrovska PN, Smith RA, Tiang T, Weinstein SR, Haupt LM, Griffiths LR. Semaphorin-plexin signalling genes associated with human breast tumourigenesis. Gene. 2011 Dec 10;489(2):63-9.
4. Monet M, Lehen'kyi V, Gackiere F, Firlej V, Vandenberghe M, Roudbaraki M, et al. Role of cationic channel TRPV2 in promoting prostate cancer migration and progression to androgen resistance. Cancer Res. 2009 Feb 1;70(3):1225-35.
5. Cowden Dahl KD, Zeineldin R, Hudson LG. PEA3 is necessary for optimal epidermal growth factor receptor-stimulated matrix metalloproteinase expression and invasion of ovarian tumor cells. Mol Cancer Res. 2007 May;5(5):413-21.
6. Boulay G, Dubuissez M, Van Rechem C, Forget A, Helin K, Ayrault O, et al. Hypermethylated in cancer 1 (HIC1) recruits polycomb repressive complex 2 (PRC2) to a subset of its target genes through interaction with human polycomb-like (hPCL) proteins. J Biol Chem. 2011 Mar 23;287(13):10509-24.

Supplementary Figure S9 Tian et al.

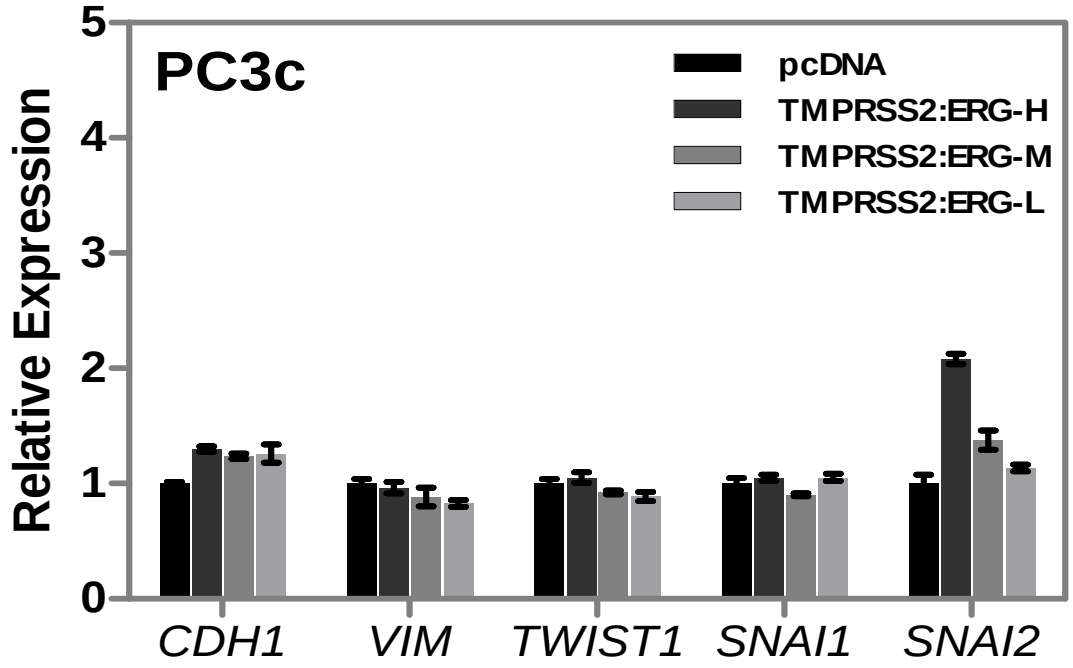

Supplementary Figure S8 Tian et al.

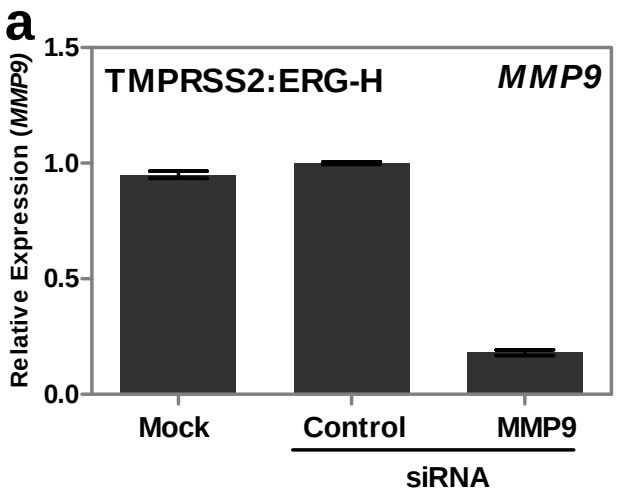

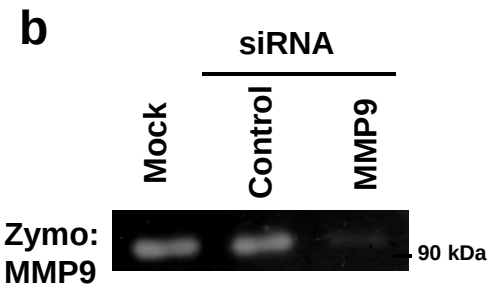

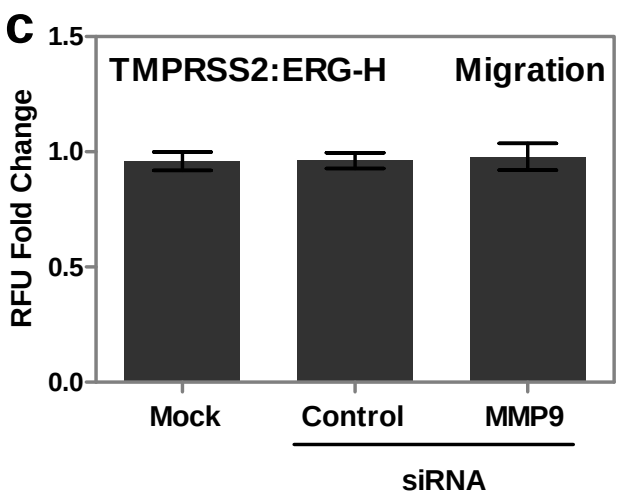

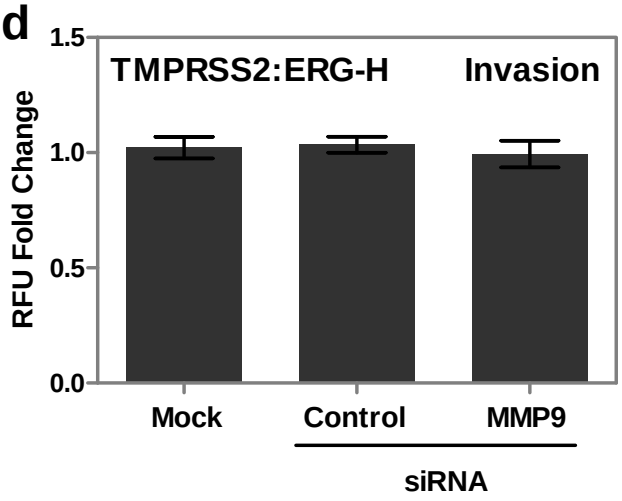

Supplementary Figure S7 Tian et al.

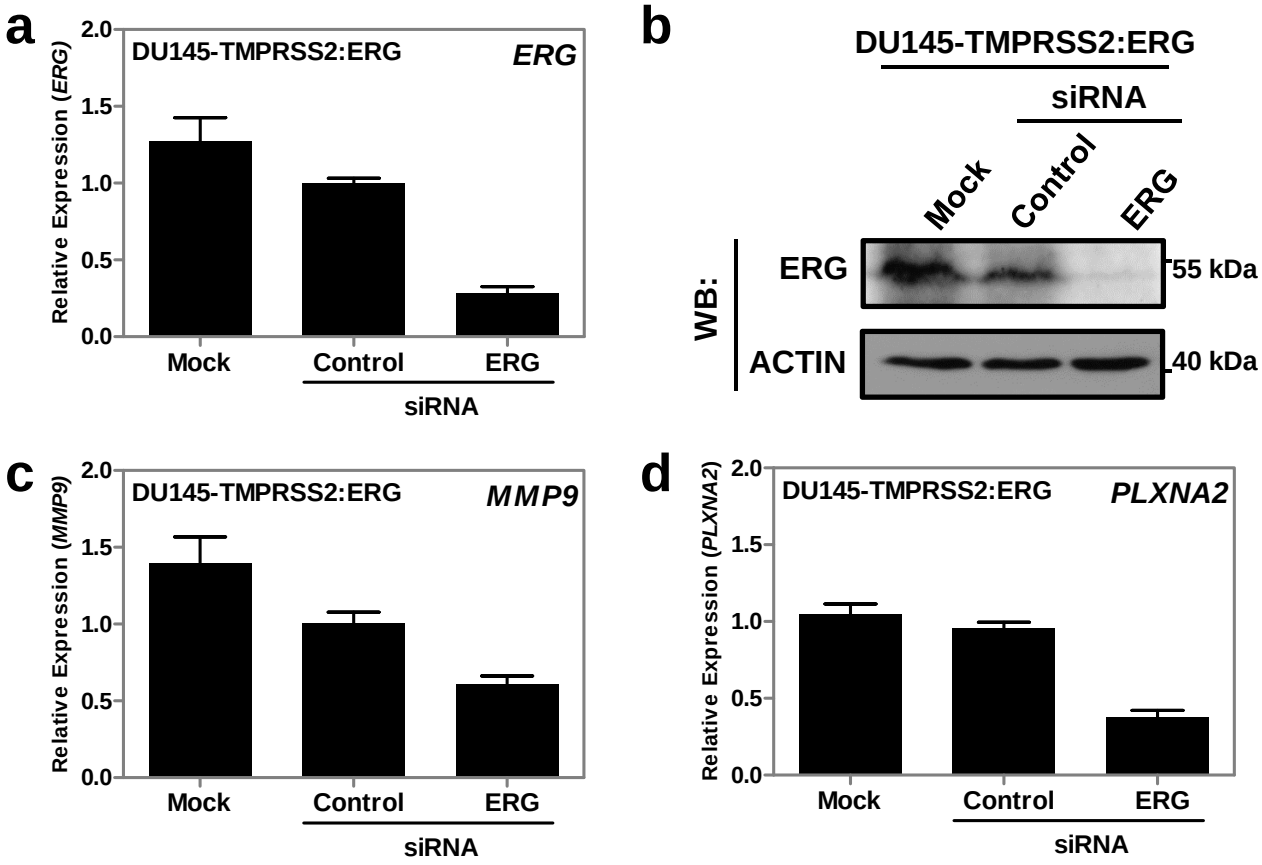

Supplementary Figure S6 Tian et al.

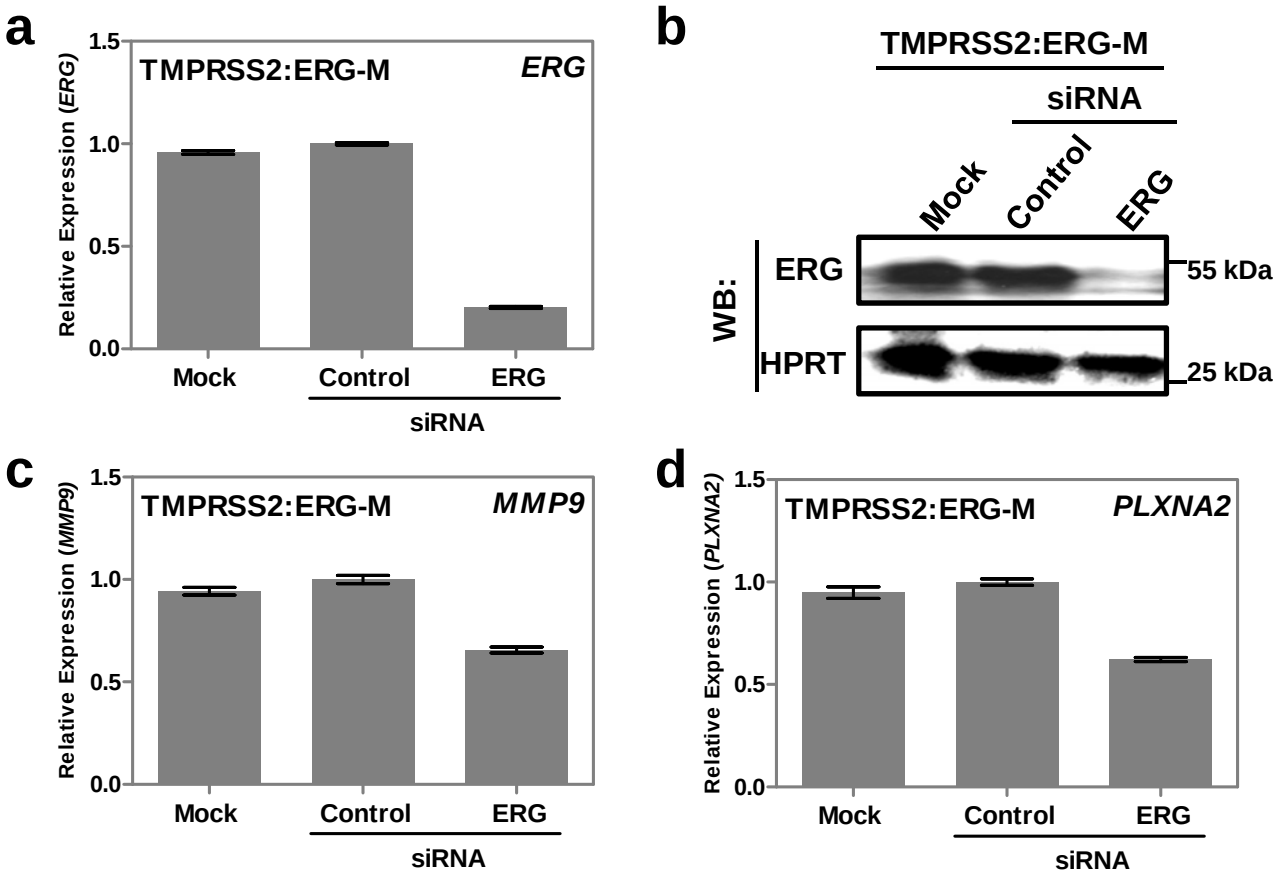

Supplementary Figure S5 Tian et al.

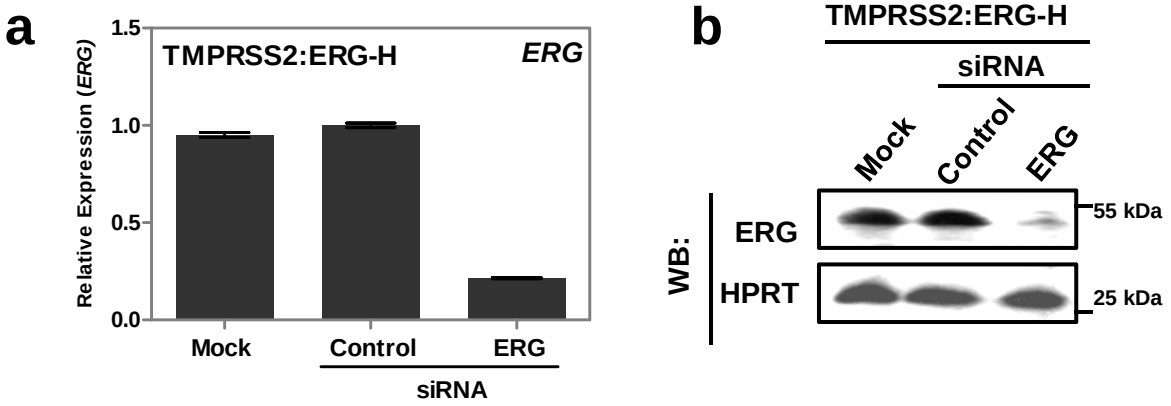

Supplementary Figure S4 Tian et al.

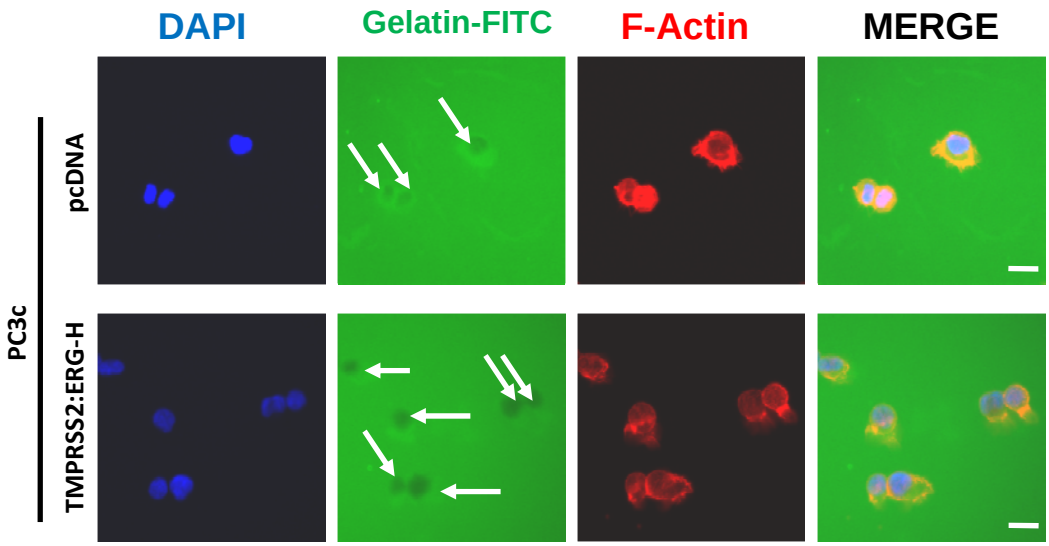

Supplementary Figure S3 Tian et al.

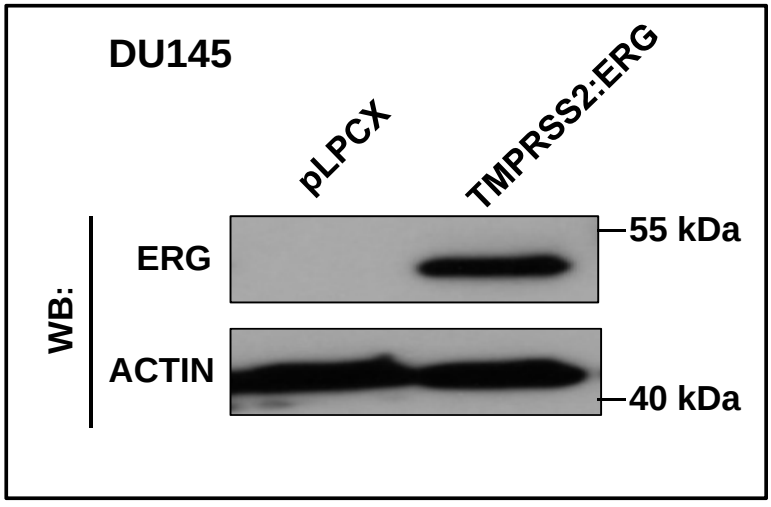

Supplementary Figure S2 Tian et al.

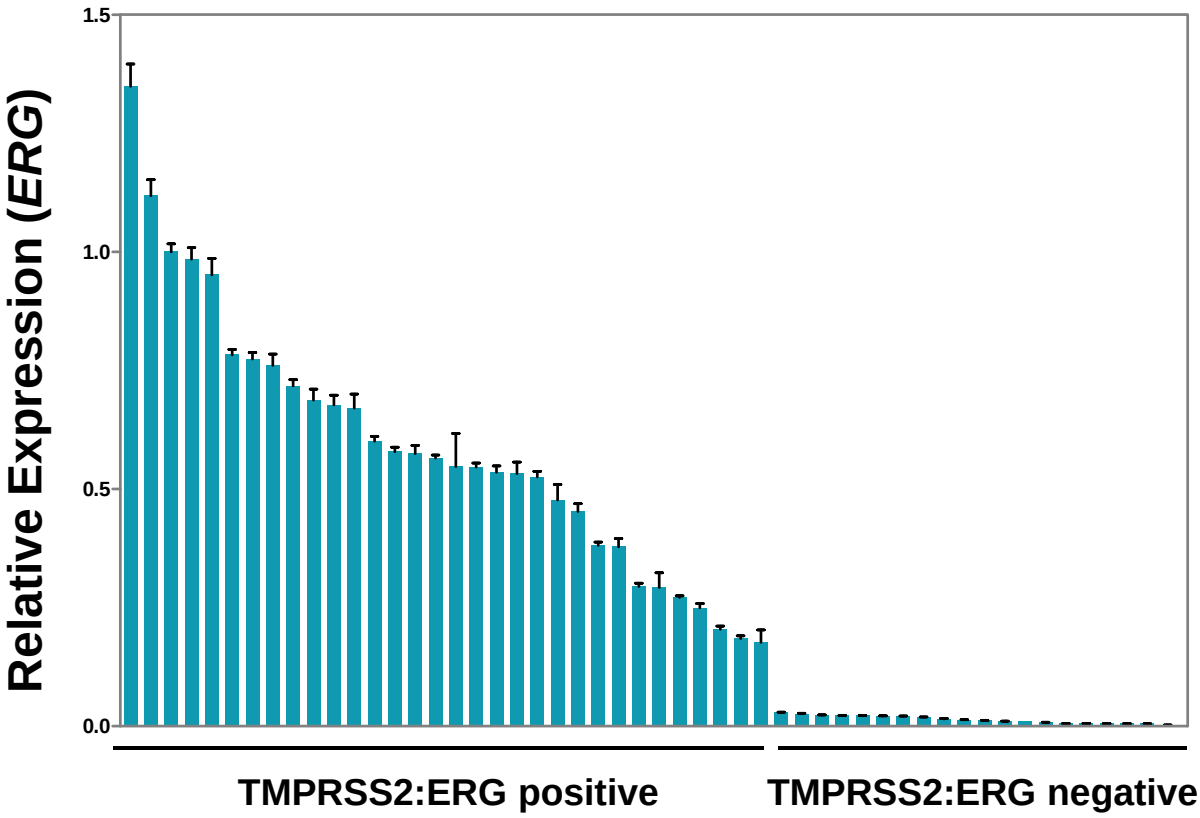

Supplementary Figure S1 Tian et al.